Journal of Sound and Vibration (2000) **233**(4), 669–705
doi:10.1006/jsvi.2000.2836, available online at http://www.idealibrary.com on IDEAL®

ESTIMATION OF ACOUSTIC SOURCE STRENGTH BY INVERSE METHODS: PART II, EXPERIMENTAL INVESTIGATION OF METHODS FOR CHOOSING REGULARIZATION PARAMETERS

S. H. Yoon and P. A. Nelson

Institute of Sound and Vibration Research, University of Southampton, Southampton SO17 1BJ, England

(*Received* 23 *October* 1998, *and in final form* 15 *December* 1999)

Two regularization methods, Tikhonov regularization and singular value discarding, are used to improve the accuracy of reconstruction of acoustic source strength by inverse techniques. In this paper, some methods are investigated for choosing the Tikhonov regularization parameter and the singular values to be discarded. Of these, we concentrate on the use of ordinary cross-validation and generalized cross-validation. These methods can provide an appropriate regularization parameter without prior knowledge of either the acoustic source strength or the contaminating measurement noise. Some experimental results obtained using a randomly vibrating simply supported plate mounted in a baffle are presented to illustrate the performance of the methods for choosing the regularization parameters.

1. INTRODUCTION

In the reconstruction of acoustic source strength by inverse techniques, the accuracy of reconstruction is largely determined by the conditioning of the matrix to be inverted. This matrix can often be ill-conditioned. This can occur despite the choice of geometrical arrangement of microphones being made to account for the behaviour of the condition number of the acoustic transfer function matrix. This is described in full in reference [1]. For example, when we wish to identify the contribution to the total acoustic field made by a vibrating surface (e.g., a plate-like structure excited by dynamic forces) from the viewpoint of a discrete inverse problem, this surface has to be discretized into a large number of small elements each of which is regarded as an acoustic source. In this case, we need also a large number of microphones, which is at least equal to the number of acoustic sources. However, such a system can result in ill-conditioning because the condition number of the matrix to be inverted increases as the dimension of this matrix increases. This ill-conditioning makes the problem ill-posed. In the ill-conditioned problem, finding a good estimate of acoustic source strength by the least-squares method becomes problematic. This is because the effect of measurement noise and/or modelling error appears in the reconstructed acoustic source strength, giving a large deviation from the desired values [1]. For this reason, we demonstrated in reference [1] that Tikhonov regularization and singular value discarding could be used to enhance the accuracy of reconstruction of acoustic source strength. In this case, the success of these regularization methods depends on the appropriate choice of the Tikhonov regularization parameter and the singular values to be discarded.

0022-460X/00/240669 + 37 $35.00/0

This paper deals with the methods for choosing these values. We introduce the techniques of ordinary cross-validation and generalized cross-validation for choosing the Tikhonov regularization parameter and the singular values to be discarded. These methods have mainly been applied in the field of statistical data analysis and image restoration (see references [2,3] for example). The main advantage of these techniques is that they do not require prior knowledge of the source strengths to be reconstructed or the contaminating noise and thus they can be used in practical situations. The theoretical basis for these methods are developed in order to obtain the formulae which enable the acoustic source strengths to be recovered with improved accuracy.

In order to explore the main features of the theories presented, we undertake a series of experiments in which we reconstruct the volume velocities of a randomly vibrating simply supported plate mounted in a baffle. The initial restoration of acoustic source strengths is conducted for "well conditioned" problems. Finally, we explore the performance of Tikhonov regularization and singular value discarding and incorporate the generalized cross-validation technique for choosing the regularization parameter and the singular values to be discarded when the inversion problem is very poorly conditioned.

2. METHODS FOR CHOOSING THE TIKHONOV REGULARIZATION PARAMETER

2.1. INTRODUCTION

In reference [1], we showed that the Tikhonov regularized solution for the acoustic source strength vector could be written as

$$\mathbf{q}_R = (\mathbf{H}^H\mathbf{H} + \beta\mathbf{I})^{-1}\mathbf{H}^H\hat{\mathbf{p}}, \tag{1}$$

where we have used the subscript R to denote "Tikhonov regularized". In this solution $\mathbf{H}$ is the matrix of acoustic transfer functions relating the vector $\mathbf{p}$ of desired (or modelled) acoustic pressures to the vector $\mathbf{q}$ of desired (or modelled) acoustic source strengths and $\hat{\mathbf{p}}$ is the vector of measured acoustic pressures. The regularization parameter is denoted by β. Similarly, we showed that for acoustic sources having a stationary random time history, the Tikhonov regularized solution for the source strength cross-spectral matrix could be written as

$$\mathbf{S}_{qqR} = \{(\mathbf{H}^H\mathbf{H} + \beta\mathbf{I})^{-1}\mathbf{H}^H)\mathbf{S}_{\hat{p}\hat{p}}\{(\mathbf{H}^H\mathbf{H} + \beta\mathbf{I})^{-1}\mathbf{H}^H\}^H, \tag{2}$$

where $\mathbf{S}_{\hat{p}\hat{p}}$ is the matrix of cross-spectra of measured acoustic pressures. In this paper, we first describe established techniques for choosing β in the solution for source strength given by equation (1). We then proceed to apply the same techniques to the solution given by equation (2) on the grounds that a good solution for $\mathbf{q}_R$ will lead to a good solution or $\mathbf{S}_{qqR}$.

In applying Tikhonov regularization, we have to consider two factors: the manner by which the result should be regularized and the amount of regularization. The method of regularization will be determined by the choice of "regularization operator" which here is chosen as the identity matrix $\mathbf{I}$, although this can be replaced by a number of linear matrix operators. Also, the degree of regularization is determined by the regularization parameter β. We shall here concentrate on only the method for choosing the regularization parameter. Further discussion regarding the choice of the regularization operator is given in reference [3]. The choice of a good value of regularization parameter in Tikhonov regularization has

received a great deal of attention [2–8]. Here we will introduce some established methods with the modifications necessary to enable them to be oriented towards our problem. In order to compare these methods we will use a simple measure of mean square error between the desired solution $\mathbf{q}$ and the regularized solution $\mathbf{q}_R(\beta)$. This is defined by

$$MSE(\beta) = E[\|\mathbf{q} - \mathbf{q}_R(\beta)\|^2]. \tag{3}$$

Similarly, in reconstructing cross-spectra we can consider the residual between the true value $\mathbf{S}_{qq}$ and the regularized solution given by

$$\mathbf{R}_{qq}(\beta) = \|\mathbf{S}_{qq} - \mathbf{S}_{qqR}(\beta)\|_e, \tag{4}$$

where $\| \ \|_e$ denotes the Euclidean norm of a matrix. Obviously, the choice of β that could be considered optimal would minimize these functions, but these of course cannot be computed in practice without prior knowledge of $\mathbf{q}$ or $\mathbf{S}_{qq}$ [3].

2.2. ORDINARY CROSS-VALIDATION

Several methods not requiring prior knowledge of either of the value to be restored or the noise have been proposed in determining the regularization parameter, such as the cross-validation technique [4], the generalized cross-validation technique [2], the L-curve method [7], and the maximum likelihood method [8]. However, here we focus on the use of the cross-validation technique and the generalized cross-validation technique. Allen [4] proposed a method, called *Allen's PRESS* (which stands for predicted sum of squares), in order to select a good ridge parameter in ridge regression analysis. This parameter is tantamount to the regularization parameter in our problem. This method usually referred to as the ordinary cross-validation (OCV) technique. This was also suggested by Wahba and Wold [9] in the context of smoothing splines. This is a widely recognized method in the field of statistical data analysis.

The essence of the method, when viewed in the current context, is to first find the vector of complex acoustic source strengths $\mathbf{q}_R(\beta, k)$ which minimizes the cost function

$$J(\beta, k) = \sum_{\substack{m=1 \\ m \neq k}}^{M} [\hat{p}_m - p_m]^2 + \beta \mathbf{q}^{\mathrm{H}}\mathbf{q}, \tag{5}$$

which is the usual cost function for minimization as described in reference [1], but with the kth values of measured and modelled pressures ($\hat{p}_k$ and p_k) omitted from the calculation. (In this sense the ordinary cross-validation technique is also sometimes referred to as "the leaving-one-out method".) Having arrived at the source strength vector $\mathbf{q}_R(\beta, k)$ that minimizes this function, we then evaluate the effectiveness of this vector in predicting the value of the measured pressure $\hat{p}_k$ that was "left out" of the calculation of the cost function. We denote the predicted value of $\hat{p}_k$ by $p_k(\beta, k)$ which is the kth component of $\mathbf{H}\mathbf{q}_R(\beta, k)$. The ordinary cross-validation function $V_0(\beta)$ is then defined in order to measure the success of this prediction when the "leaving-one-out" process is repeated for all the available data points $\hat{p}_k$ (i.e., for $k = 1$ to M). The ordinary cross-validation function is thus defined by

$$V_0(\beta) = \frac{1}{M} \sum_{k=1}^{M} [\hat{p}_k - p_k(\beta, k)]^2. \tag{6}$$

The value of β which leads to the minimization of this function is then deemed "optimal"; it is the value of the regularization parameter β which ensures the best prediction of each of the measured pressures from knowledge of all the other measured pressures.

A notationally convenient means for expressing this cost function can also be developed by following the procedure presented by Craven and Wahba [10]. One first has to recognize that the solution to the minimization of $J(\beta, k)$ can be found by solving the full M-point minimization problem but with the data point $\hat{p}_k$ given by the kth component of the solution to the problem, i.e., we set $\hat{p}_k = p_k(\beta, k)$. A rigorous proof of this observation is given by Craven and Wahba [10]. Here we illustrate this method of approach and write the cost function given by equation (5) as

$$J(\beta, k) = [\hat{\mathbf{p}}(k) - \mathbf{p}]^{\mathrm{H}}[\hat{\mathbf{p}}(k) - \mathbf{p}] + \beta \mathbf{q}^{\mathrm{H}}\mathbf{q}, \tag{7}$$

where the vector of measured pressures $\hat{\mathbf{p}}(k)$ is given by

$$\hat{\mathbf{p}}^{\mathrm{T}}(k) = [\hat{p}_1 \hat{p}_2 \cdots \hat{p}_{k-1} p_k(\beta, k) \hat{p}_{k+1} \cdots \hat{p}_M]. \tag{8}$$

The solution for the source strength vector $\mathbf{q}_R(\beta, k)$ that minimizes this function is given by

$$\mathbf{q}_R(\beta, k) = (\mathbf{H}^{\mathrm{H}}\mathbf{H} + \beta \mathbf{I})^{-1}\mathbf{H}^{\mathrm{H}}\hat{\mathbf{p}}(k). \tag{9}$$

Thus, we can write the vector of estimated pressures that minimize $J(\beta, k)$ as

$$\mathbf{p}(\beta, k) = \mathbf{H}\mathbf{q}_R(\beta, k) = \mathbf{H}(\mathbf{H}^{\mathrm{H}}\mathbf{H} + \beta \mathbf{I})^{-1}\mathbf{H}^{\mathrm{H}}\hat{\mathbf{p}}(k) = \mathbf{B}(\beta)\hat{\mathbf{p}}(k), \tag{10}$$

where the matrix $\mathbf{B}(\beta)$ (the "influence matrix") is given by $\mathbf{H}(\mathbf{H}^{\mathrm{H}}\mathbf{H} + \beta \mathbf{I})^{-1}\mathbf{H}^{\mathrm{H}}$. This relationship, when written in full, thus takes the form

$$\begin{bmatrix} p_1(\beta, k) \\ p_2(\beta, k) \\ \vdots \\ p_k(\beta, k) \\ \vdots \\ p_M(\beta, k) \end{bmatrix} = \begin{bmatrix} b_{11} & b_{12} & \cdots & b_{1M} \\ b_{21} & b_{22} & \cdots & b_{2M} \\ \vdots & \vdots & & \vdots \\ b_{k1} & b_{k2} & \cdots & b_{kM} \\ \vdots & \vdots & & \vdots \\ b_{M1} & b_{M2} & \cdots & b_{MM} \end{bmatrix} \begin{bmatrix} \hat{p}_1 \\ \hat{p}_2 \\ \vdots \\ p_k(\beta, k) \\ \vdots \\ \hat{p}_M \end{bmatrix}. \tag{11}$$

where b_{ij} are the components of matrix $\mathbf{B}(\beta)$. Now note that the solution to the M-point minimization problem with no changes made to the vector of measured pressures $\hat{\mathbf{p}}$ can be written as

$$\mathbf{q}_R(\beta) = (\mathbf{H}^{\mathrm{H}}\mathbf{H} + \beta \mathbf{I})^{-1}\mathbf{H}^{\mathrm{H}}\hat{\mathbf{p}} \tag{12}$$

and thus the corresponding set of estimated pressures can be written as $\mathbf{p}(\beta) = \mathbf{H}\mathbf{q}_R(\beta) = \mathbf{B}(\beta)\hat{\mathbf{p}}$. When written in full, this relationship can be expressed as

$$\begin{bmatrix} p_1(\beta) \\ p_2(\beta) \\ \vdots \\ p_k(\beta) \\ \vdots \\ p_M(\beta) \end{bmatrix} = \begin{bmatrix} b_{11} & b_{12} & \cdots & b_{1M} \\ b_{21} & b_{22} & \cdots & b_{2M} \\ \vdots & \vdots & & \vdots \\ b_{k1} & b_{k2} & \cdots & b_{kM} \\ \vdots & \vdots & & \vdots \\ b_{M1} & b_{M2} & \cdots & b_{MM} \end{bmatrix} \begin{bmatrix} \hat{p}_1 \\ \hat{p}_2 \\ \vdots \\ \hat{p}_k \\ \vdots \\ \hat{p}_M \end{bmatrix}. \tag{13}$$

From the above two matrix expressions we can derive a relationship between $p_k(\beta, k)$ and $p_k(\beta)$. It follows that

$$p_k(\beta, k) = b_{k1}\hat{p}_1 + b_{k2}\hat{p}_2 + \cdots + b_{kk}p_k(\beta, k) + \cdots + b_{kM}\hat{p}_M \tag{14}$$

and also that

$$p_k(\beta) = b_{k1}\hat{p}_1 + b_{k2}\hat{p}_2 + \cdots + b_{kk}\hat{p}_k + \cdots + b_{kM}\hat{p}_M. \tag{15}$$

Taking the difference between these two equations then shows that

$$(1 - b_{kk})p_k(\beta, k) = p_k(\beta) - b_{kk}\hat{p}_k. \tag{16}$$

It therefore follows, after some algebra, that

$$\hat{p}_k - p_k(\beta, k) = \frac{\hat{p}_k - p_k(\beta)}{1 - b_{kk}}. \tag{17}$$

This enables the expressions for the ordinary cross-validation function $V_0(\beta)$ given by equation (6) to be written as

$$V_0(\beta) = \frac{1}{M}\sum_{k=1}^{M}\left[\frac{(\hat{p}_k - p_k(\beta))}{(1 - b_{kk})}\right]^2. \tag{18}$$

Note also that since $\mathbf{p}(\beta) = \mathbf{H}\mathbf{q}_R(\beta) = \mathbf{B}(\beta)\hat{\mathbf{p}}$ then we may write this expression as

$$V_0(\beta) = \frac{1}{M}\|\mathbf{C}(\mathbf{I} - \mathbf{B}(\beta))\hat{\mathbf{p}}\|_e^2, \tag{19}$$

where $\mathbf{C}$ is the diagonal matrix whose entries are also given by $1/(1 - b_{kk})$. Note that $V_0(\beta)$ is not a function of either the source strength to be restored or the noise but a function of only $\mathbf{H}$ the assumed transfer function matrix, $\hat{\mathbf{p}}$ the measured pressure vector, and, of course, β the regularization parameter. We denote the value of β that minimizes the function $V_0(\beta)$ by β_{OCV}.

2.3. GENERALIZED CROSS-VALIDATION

It was pointed out by Golub *et al.* [2] that the ordinary cross-validation technique described above may be expected to fail in cases where the matrix $\mathbf{B}(\beta)$ is close to diagonal. It is clear that if $\mathbf{B}(\beta)$ is diagonal, then the cross-validation function $V_0(\beta)$ given above reduces simply to $(1/M)\|\hat{\mathbf{p}}\|_e^2$ (i.e., $1/M$ times the sum of squared measured pressures) which is entirely independent of the choice of β. This shortcoming led Golub *et al.* [2] to suggest the use of "generalized cross-validation" (GCV) which follows from their argument that any good choice of β should be "invariant under rotation of the measurement co-ordinate system". Here we follow the analysis put forward by Golub *et al.* in deriving the GCV function appropriate to the case considered here.

Firstly, we employ the singular value decomposition (SVD) of the matrix $\mathbf{H}$ [1] to write the relationship $\hat{\mathbf{p}} = \mathbf{H}\mathbf{q} + \mathbf{e}$ in the form

$$\hat{\mathbf{p}} = \mathbf{U}\mathbf{\Sigma}\mathbf{V}^{\mathrm{H}}\mathbf{q} + \mathbf{e} \tag{20}$$

and since the unitary matrix $\mathbf{U}$ has the property $\mathbf{U}^{\mathrm{H}}\mathbf{U} = \mathbf{I}$, then pre-multiplication of this equation by $\mathbf{U}^{\mathrm{H}}$ results in

$$\mathbf{U}^{\mathrm{H}}\hat{\mathbf{p}} = \mathbf{\Sigma}\mathbf{V}^{\mathrm{H}}\mathbf{q} + \mathbf{U}^{\mathrm{H}}\mathbf{e}. \tag{21}$$

Note that this equation describes the relationship between the "transformed" pressure $\tilde{\mathbf{p}} = \mathbf{U}^{\mathrm{H}}\hat{\mathbf{p}}$ and the "transformed" source strength $\tilde{\mathbf{q}} = \mathbf{V}^{\mathrm{H}}\mathbf{q}$ as described in reference [1]. This equation is further transformed by pre-multiplication by the matrix $\mathbf{W}$ which has the ikth entry given by

$$W_{ik} = \frac{1}{\sqrt{M}}\,\mathrm{e}^{2\pi \mathrm{j} ik/M}, \quad i, k = 1, 2, \ldots, M, \tag{22}$$

where $\mathrm{j} = \sqrt{-1}$. The matrix $\mathbf{W}$ is a unitary matrix ($\mathbf{W}^{\mathrm{H}}\mathbf{W} = \mathbf{I}$) and has the effect of applying a discrete Fourier transform to the vectors $\mathbf{U}^{\mathrm{H}}\hat{\mathbf{p}}$, etc. appearing in equation (21). This then becomes

$$\mathbf{W}\mathbf{U}^{\mathrm{H}}\hat{\mathbf{p}} = \mathbf{W}\mathbf{\Sigma}\mathbf{V}^{\mathrm{H}}\mathbf{q} + \mathbf{W}\mathbf{U}^{\mathrm{H}}\mathbf{e}. \tag{23}$$

The transformed model is thus written as

$$\hat{\mathbf{p}}_{trans} = \mathbf{H}_{trans}\mathbf{q}_{trans} + \mathbf{e}_{trans}, \tag{24}$$

where $\mathbf{p}_{trans} = \mathbf{W}\mathbf{U}^{\mathrm{H}}\hat{\mathbf{p}}$ is the vector of transformed measured pressures, $\mathbf{q}_{trans} = \mathbf{W}\mathbf{V}^{\mathrm{H}}\mathbf{q}$ is the vector of transformed source strengths, $\mathbf{e}_{trans} = \mathbf{W}\mathbf{U}^{\mathrm{H}}\mathbf{e}$ is the vector of transformed noise components and $\mathbf{H}_{trans} = \mathbf{W}\mathbf{\Sigma}\mathbf{W}^{\mathrm{H}}$.

The procedure adopted by Golub *et al.* is then to apply ordinary cross-validation to this transformed model. Firstly, the transformed influence matrix $\mathbf{B}_{trans}$ is defined by $\mathbf{H}_{trans}(\mathbf{H}_{trans}^{\mathrm{H}}\mathbf{H}_{trans} + \beta\mathbf{I})^{-1}\mathbf{H}_{trans}^{\mathrm{H}}$ and $\hat{\mathbf{p}}_{trans}$ is substituted into the expression for the ordinary cross-validation function given by equation (19). Noting that $\mathbf{B}_{trans}$ is a circulant matrix [11] and thus constant down the diagonals then shows that the generalized cross-validation function can be written as

$$V(\beta) = \frac{(1/M)\,\|(\mathbf{I} - \mathbf{B}_{trans})\hat{\mathbf{p}}_{trans}\|_e^2}{[(1/M)\mathrm{Tr}(\mathbf{I} - \mathbf{B}_{trans})]^2}, \tag{25}$$

where Tr denotes the trace (sum of diagonal entries) of a matrix. By expressing $V(\beta)$ in terms of the eigenvalues of $\mathbf{B}_{trans}$ and noting that these are the same as the eigenvalues of $\mathbf{B}(\beta)$ (see Golub *et al.* [2]) also shows that the generalized cross-validation function can be written as

$$V(\beta) = \frac{(1/M)\,\|\mathbf{I} - \mathbf{B}(\beta))\hat{\mathbf{p}}\|_e^2}{[(1/M)\mathrm{Tr}(\mathbf{I} - \mathbf{B}(\beta))]^2}. \tag{26}$$

Furthermore, it can be shown [12] that $V(\beta)$ is a weighted version of the ordinary cross-validation function $V_0(\beta)$ (equation (6)) such that

$$V(\beta) = \frac{1}{M}\sum_{k=1}^{M}\left[\frac{(\hat{p}_k - p_k(\beta))}{(1 - b_{kk})}\right]^2 w_{kk}, \tag{27}$$

where

$$w_{kk} = \left(\frac{(1 - b_{kk})}{1 - (1/M)\,\mathrm{Tr}\,\mathbf{B}(\beta)}\right)^2. \tag{28}$$

Note that the term $(1/M)\mathrm{Tr}\,\mathbf{B}(\beta)$ evaluates the average of the sum of all diagonal elements of the influence matrix $\mathbf{B}(\beta)$. Thus, the weighting factor $w_{kk}(\beta)$ represents the contribution of each diagonal element relative to the sum of all diagonal elements of $\mathbf{B}(\beta)$. The generalized cross-validatory choice of the regularization parameter β_{GCV} is made by minimizing the function $V(\beta)$. Also note that when $\mathbf{B}$ is a circulant matrix (i.e., when $\mathbf{H}$ is circulant), $V(\beta)$ is identical to $V_0(\beta)$ since in this case $w_{kk} = 1$. Finally, consider the denominator and numerator of the function $V(\beta)$. The denominator is given by $[(1/M)\mathrm{Tr}[\mathbf{I} - \mathbf{H}(\mathbf{H}^H\mathbf{H} + \beta\mathbf{I})^{-1}\mathbf{H}^H]]^2$ and thus evaluates the perturbation in the matrix $\mathbf{H}^H\mathbf{H}$ caused by the presence of regularization parameter in improving the conditioning of the matrix $\mathbf{H}^H\mathbf{H}$. As β is increased, the denominator will become progressively smaller than unity, thus tending to increase $V(\beta)$. Also, the numerator is given by $(1/M)\|\hat{\mathbf{p}} - \mathbf{H}\mathbf{q}_R(\beta)\|_e^2$ and thus represents the residual sum of squares. Therefore, the function $V(\beta)$ evaluates both the error in the solution and the inaccuracy introduced into the matrix to be inverted by the inclusion of the regularization parameter.

In closing this section it should be mentioned that the GCV technique does not always produce satisfactory results. Some workers have made cautionary remarks as to the use of this technique. Wahba [12] stated that the GCV was quite likely to produce an unsatisfactory result if the noise components contaminating the measured data are highly correlated. This is a reflection of the basic assumption regarding the noise made at the starting point of the derivation of $V(\beta)$ [2], in which the noise components are assumed to be independent and identically distributed, with zero mean and the same variance. In addition, from a simulation study, Thompson *et al.* [13] showed some empirical evidence of the possibilities for the unsatisfactory choice of the regularization parameter when the GCV technique is employed. They stated that the potential problems with the $V(\beta)$ function fall into one or a combination of the following groups: $V(\beta)$ with multiple minima, $V(\beta)$ with no minimum for $\beta > 0$, $V(\beta)$ for which it is hard to locate the global minimum numerically, and $V(\beta)$ whose global minimum produces an unsatisfactory β_{GCV}. It is therefore desirable to bear these points in mind when using the GCV technique.

2.4. AN EXAMPLE OF THE APPLICATION OF CROSS-VALIDATION TECHNIQUES

By way of introduction to the use of these techniques, we illustrate their use with a simple model (Figure 1). This consists of a line array of nine-point monopole sources and a line array of nine microphones. It is assumed that only the source located centrally has unit volume velocity (say 1 m^3/s) and 10% measurement noise is added to acoustic pressures sensed at the microphones. The graphs of Figure 2 show the values of functions $MSE(\beta)$, $V_0(\beta)$ and $V(\beta)$ defined by equations (3), (19) and (26) plotted against the regularization parameters for the cases in which the source-to-microphone distance (r_{ms}) is different. The first row in Figure 2 shows the results of the simulation when the microphone array is placed very close to the source array ($r_{ms} = 0{\cdot}5r_{ss}$). As a consequence, the problem is very well conditioned and there is no real need for regularization and $MSE(\beta)$ is in any case very small. The second, third and fourth rows show the results as the microphone array is moved progressively further away from the source array ($r_{ms} = 2r_{ss}, 3r_{ss}, 30r_{ss}$) and in these cases, clear minima are observed in the functions $V_0(\beta)$ and $V(\beta)$ (corresponding roughly to values of β of 10^{-3}, 10^{-4} and 10^{-5}). In all three cases, the values of β that minimize $V(\beta)$ are similar to those that minimize $V_0(\beta)$. In none of the cases is there a clear correspondence between the behaviour of $MSE(\beta)$ with $V(\beta)$ and $V_0(\beta)$, although in the second and third rows of results $MSE(\beta)$ obviously increases once the optimal values of β exceeded.

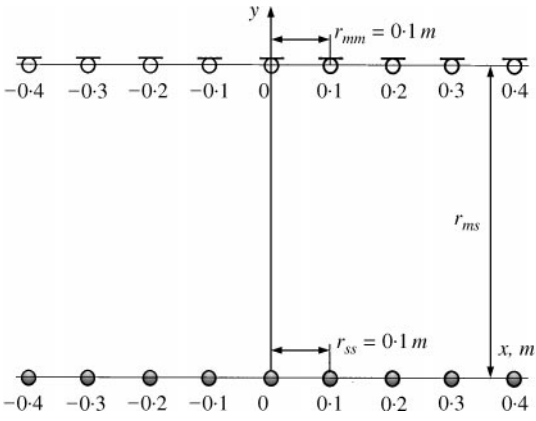

Figure 1. A geometrical arrangement of nine point monopole sources and nine microphones.

It is of course impossible to draw general conclusions from the results of this illustrative simulation, but it does at least demonstrate that for the type of case considered here, clear minima of $V_0(\beta)$ and $V(\beta)$ do exist and that the values deduced have the correct order of magnitude. Again, although in these cases there are no clear differences between the behaviour of $V_0(\beta)$ and $V(\beta)$, we shall generally continue to use the generalized cross-validation function $V(\beta)$ since its superiority has been thoroughly argued by other workers [2,10]. Furthermore, we will demonstrate with the experimental results presented below, that the use of the GCV function $V(\beta)$ is highly effective in restoring the strength of acoustic sources when the inverse problem is badly conditioned.

2.5. ALGORITHMS FOR DETERMINATION OF OPTIMAL REGULARIZATION PARAMETERS

Finally, note that we can also use the function $V(\beta)$ in order to reconstruct source strength auto- and cross-spectra on the grounds that a regularization parameter producing a satisfactory recovery of $\mathbf{q}$ should also yield a good reconstruction of $\mathbf{S}_{qq}$. Accordingly, after estimating the regularization parameter based on the minimization of the function $V(\beta)$ given by equation (26), we substitute this into equation (2). In order to compare the results of the application of GCV to the determination of the optimally regularized solution, we use the algorithm depicted in Figure 3 in order to determine the minimum of R_{qq} defined in equation (4). We also employ the procedure shown in Figure 4 as an algorithm for identifying β_{GCV}. This procedure is similar to that providing β_{qq} of Figure 3. We first read $\mathbf{H}(\omega)$ and $\hat{\mathbf{p}}(\omega)$ at the lower frequency ω_l of interest. Then the first trial regularization parameter is given by the initial weight W_i multiplied by the minimum singular value of $\mathbf{H}^{\mathrm{H}}\mathbf{H}$. Using these data, the value of the generalized cross-validation function $V(\beta)$ is computed. After that, $V(\beta)$ is recursively computed by successively changing the value of weight W by a suitable stepsize ΔW from the initial value W_i to the final value W_f. From the values of $V(\beta)$, we find a particular β which produces the minimum $V(\beta)$. At this point, the value β becomes the regularization parameter β_{GCV} which we wish to identify. Using the selected β_{GCV}, we eventually obtain $\mathbf{S}_{qqR}$. This process is repeated until the upper frequency ω_u of interest.

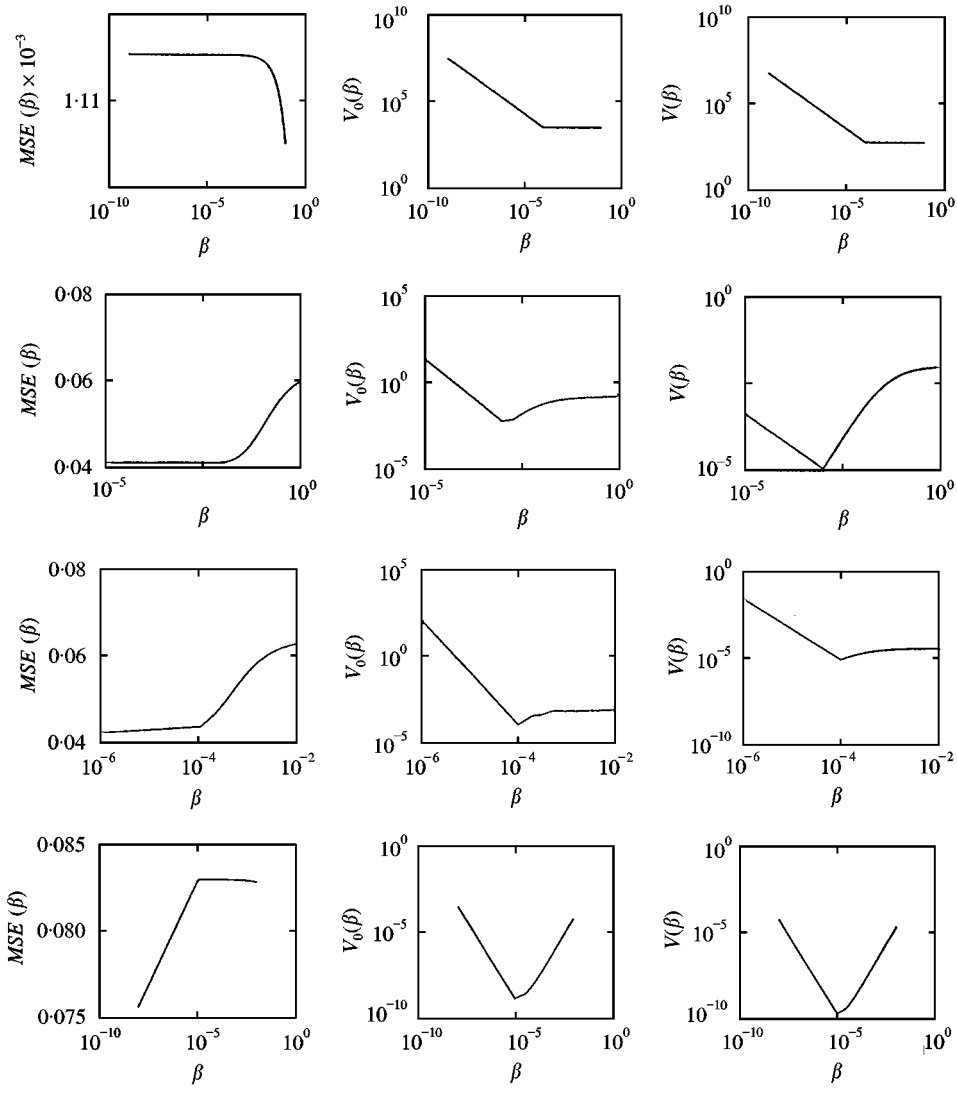

Figure 2. Comparison of (a) $MSE\ (\beta)$, (b) $V_0(\beta)$ and (c) $V(\beta)$ for the model of Figure 1: $r_{ms} = 0{\cdot}5r_{ss}$ (the 1st row), $2r_{ss}$ (the 2nd row), $3r_{ss}$ (the 3rd row), $30r_{ss}$ (the 4th row), $r_{ss} = 0{\cdot}1$ m.

3. USE OF GENERALIZED CROSS-VALIDATION FOR SINGULAR VALUE DISCARDING

3.1. INTRODUCTION

The singular value discarded solution estimating the vector of acoustic source strength is given by [1]

$$\mathbf{q}_D = \mathbf{H}_D^+ \hat{\mathbf{p}} = (\mathbf{V}\boldsymbol{\Sigma}_D^+ \mathbf{U}^{\mathrm{H}})\hat{\mathbf{p}}, \tag{29}$$

where $\mathbf{U}$ and $\mathbf{V}$ are the matrices consisting of the left and right singular vectors of $\mathbf{H}$, $\boldsymbol{\Sigma}_D$ is the matrix of singular values remaining after discarding some singular values, the superscript $^+$ denotes the pseudo-inverse, and $\mathbf{H}_D = \mathbf{U}\boldsymbol{\Sigma}_D\mathbf{V}^{\mathrm{H}}$. Note that it is also possible to

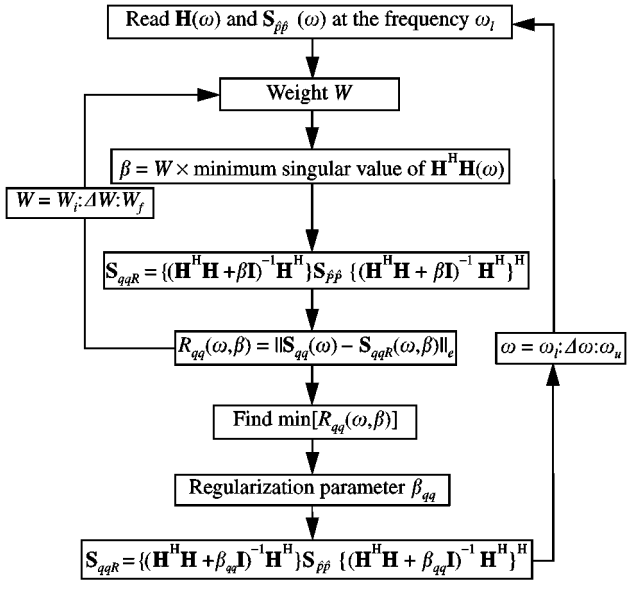

Figure 3. A method of finding the regularization parameter β_{qq} by minimizing the residual $R_{qq}(\omega, \beta)$ between the desired solution $\mathbf{S}_{qq}$ and the regularized solution $\mathbf{S}_{qqR}$.

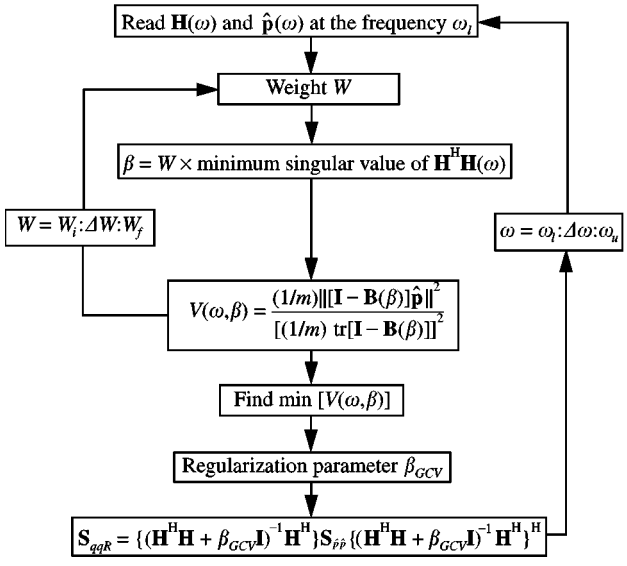

Figure 4. A method of finding the regularization parameter β_{GCV} by minimizing the generalized cross-validation function $V(\beta)$.

construct the cross-spectral matrix of acoustic source strengths from the expression

$$\mathbf{S}_{qqD} = \mathbf{H}_D^+\mathbf{S}_{\hat{p}\hat{p}}(\mathbf{H}_D^+)^H = (\mathbf{V}\boldsymbol{\Sigma}_D^+\mathbf{U}^H)\mathbf{S}_{\hat{p}\hat{p}}(\mathbf{V}\boldsymbol{\Sigma}_D^+\mathbf{U}^H)^H. \tag{30}$$

In connection with the determination of the singular values to be truncated, some researchers suggest that it is suitable to discard the singular values below "machine epsilon"

(as pointed out by Rothwell and Drachman [14], for example). However, it is important to recognize the fact that the conditioning of the matrix to be inverted is determined by not the absolute magnitudes of the singular values but the ratio of the largest to the smallest singular value. Poor conditioning can arise even if the smallest singular value is much larger than machine epsilon. It is therefore clear that this guide is not desirable. Powell and Seering [15] used the singular value discarding method when researching the problem of identifying multiple input forces (which served as sources of structural vibration) from multiple vibration measurements and the transfer functions between forces and vibration signals. In this study they rejected the singular values smaller than the error computed from coherence functions in association with the frequency response measurements. More recently, Krzanowski and Kline [16] proposed a way of determining the number of significant components in principal component analysis [17] by the use of the cross-validation technique. The principal components of principal component analysis are the same as the singular values of singular value decomposition. In this sense, the cross-validation technique used to determine the significant principal components can be applied to deciding the singular values to be eliminated in our problem.

3.2. APPLICATION OF GENERALIZED CROSS-VALIDATION

Another way to determine the singular values to be removed is through the use of GCV which was also used in choosing a good Tikhonov regularization parameter (section 2). Golub *et al.* [2] proposed the adoption of the GCV technique as a tool for choosing the significant principal components in association with principal component analysis. Consider the SVD of the $(M \times N)$ matrix $\mathbf{H}$, i.e., $\mathbf{H} = \mathbf{U}\boldsymbol{\Sigma}\mathbf{V}^{\mathrm{H}}$ in which $\mathbf{U}$ is of order $(M \times M)$, $\boldsymbol{\Sigma}$ is $(M \times N)$, and $\mathbf{V}$ is $(N \times N)$. From this matrix $\mathbf{H}$, a matrix $\mathbf{H} = \mathbf{U}\boldsymbol{\Sigma}_V\mathbf{V}^{\mathrm{H}}$ is constructed in which $\boldsymbol{\Sigma}_V$ is the $(M \times N)$ diagonal matrix consisting of the first to the vth non-zero singular values of $\mathbf{H}$ (the $(v+1)$th to the Nth singular values are set to zero). Thus,

$$\boldsymbol{\Sigma}_v = \left[\begin{array}{cccc} s_1 & & & \\ & s_2 & & 0 \\ & & \ddots & \\ & & & s_v \\ & & 0 & \\ & 0 & & \\ & & & 0 \\ \cdots\cdots & & \cdots\cdots & \\ & 0 & & \end{array}\right] \begin{array}{l} \left.\vphantom{\begin{array}{c}a\\a\\a\\a\end{array}}\right\} (v \times N) \\ \left.\vphantom{\begin{array}{c}a\\a\\a\\a\\a\\a\\a\end{array}}\right\} (N \times N) \\ \left.\vphantom{\begin{array}{c}a\\a\\a\end{array}}\right\} (M - N) \times N \end{array} \left.\vphantom{\begin{array}{c}a\\a\\a\\a\\a\\a\\a\\a\\a\end{array}}\right\} (M \times N). \tag{31}$$

Based on this matrix $\mathbf{H}_v$, we construct a matrix $\mathbf{B}_v$ defined by

$$\mathbf{B}_v = \mathbf{H}_v(\mathbf{H}_v^{\mathrm{H}}\mathbf{H}_v)^{+}\mathbf{H}_v^{\mathrm{H}}. \tag{32}$$

Note that the matrix $\mathbf{B}_v$ is similar to the influence matrix $\mathbf{B}(\beta)$ which was used in association with the determination of the regularization parameter β_{GCV}. Use of the SVD of $\mathbf{H}_v$ shows that we can write this expression in the form

$$\mathbf{B}_v = \mathbf{U}\mathbf{I}_v\mathbf{U}^{\mathrm{H}}, \tag{33}$$

where the matrix $\mathbf{I}_v$ is given by

$$\mathbf{I}_v = \mathbf{\Sigma}_v(\mathbf{\Sigma}_v^{\mathrm{H}}\mathbf{\Sigma}_v)^{+}\mathbf{\Sigma}_v^{\mathrm{H}}$$

$$= \begin{bmatrix} 1 & & & & & & \\ & 1 & & & & 0 & \\ & & \ddots & & & & \\ & & & 1 & & & \\ & & & & 0 & & \\ & & & & & \ddots & \\ & & & & & & 0 \\ \hdashline 0 & & & & 0 & & \\ & & & & & \ddots & \\ & & & & & & 0 \end{bmatrix} \left.\begin{matrix} \\ \\ \\ \\ \\ \\ \\ \\ \\ \end{matrix}\right\} (v \times N) \left.\begin{matrix} \\ \\ \\ \\ \\ \\ \\ \\ \\ \end{matrix}\right\} (N \times N) \left.\begin{matrix} \\ \\ \\ \\ \\ \\ \\ \\ \\ \end{matrix}\right\} (M \times M). \tag{34}$$

Note in this equation that the $(N+1)$th to the Mth diagonal components are originally zeros, because $\mathbf{H}$ is an $(M \times N)$ rectangular matrix and thus its singular value matrix $\mathbf{\Sigma}$ has $(M-N) \times N$ zero components as shown in equation (31). (For the case of an $(M \times M)$ square $\mathbf{H}$ matrix, there are no $(M-N) \times N$ zero components). Finally, define a function V_v of $\mathbf{B}_v$ as

$$V_v = \frac{(1/M)\|[\mathbf{I} - \mathbf{B}_v]\hat{\mathbf{p}}\|_e^2}{[(1/M)\mathrm{Tr}[\mathbf{I} - \mathbf{B}_v]]^2}, \tag{35}$$

which is the same with $V(\beta)$ given by equation (26) except that $\mathbf{B}_v$ is used instead of $\mathbf{B}(\beta)$. Golub *et al.* [2] suggested that the significant principal components could be decided by choosing $\mathbf{B}_v$ for which V_v was smallest. According to this idea, we can apply the GCV technique to the determination of the singular values to be eliminated in our problem. That is to say, we can discard some singular values as follows. At first we calculate the value of V_v by using $\mathbf{B}_v$ in which all diagonal components of $\mathbf{I}_v$ are unity except the Nth diagonal component set equal to zero. Then the same calculation is undertaken again by using another $\mathbf{B}_v$ where the $(N-1)$th and Nth diagonal components of $\mathbf{I}_v$ are replaced by zeros. This process is repeated up to the case of $\mathbf{B}_v$ in which the third to the Nth diagonal components of $\mathbf{I}_v$ are set to zero. After that, among the calculated values (i.e., $N-2$) of V_v, we find the minimum. Finally, the number of the smallest singular values to be discarded from the matrix $\mathbf{H}$ is made equal to the number of zeros contained in the first to the Nth diagonal components of the matrix $\mathbf{I}_v$ associated with the minimum value of V_v. Also note that using the properties of trace of the matrix [11], we can express $\mathrm{Tr}[\mathbf{I} - \mathbf{B}_v] = \mathrm{Tr}[\mathbf{I}] - \mathrm{Tr}[\mathbf{B}_v]$, $\mathrm{Tr}[\mathbf{I}] = M$ (where $\mathbf{I}$ is M-dimensional identity matrix), and $\mathrm{Tr}[\mathbf{B}_v] = \mathrm{Tr}[\mathbf{U}\mathbf{I}_v\mathbf{U}^{\mathrm{H}}] = \mathrm{Tr}[\mathbf{I}_v\mathbf{U}^{\mathrm{H}}\mathbf{U}] = \mathrm{Tr}[\mathbf{I}_v] = v$. Thus, equation (35) can be written as

$$V_v = \frac{(1/M)\|[\mathbf{I} - \mathbf{B}_v]\hat{\mathbf{p}}\|_e^2}{[1 - v/M]^2}. \tag{36}$$

The denominator of this expression evaluates the inaccuracy caused by discarding singular values to improve the conditioning of matrix $\mathbf{H}$. Also, the numerator evaluates the residual sum of squares produced by the perturbation in the matrix $\mathbf{H}$, since this is given by $(1/M)\|[\mathbf{I} - \mathbf{H}_v(\mathbf{H}_v^{\mathrm{H}}\mathbf{H}_v)^{+}\mathbf{H}_v^{\mathrm{H}}]\hat{\mathbf{p}}\|_e^2$. It is therefore clear that the function V_v determines the

singular values to be discarded by considering both these factors in a similar way to the GCV function above.

Another possible discarding technique is based on the singular value distribution. That is to say, the determination of the singular values to be removed is made simply by looking into the relative magnitude of the singular values. Thus, this method demands empirical experience to some extent. This utilizes only the singular value distribution obtainable from the transfer function matrix $\mathbf{H}$. We will refer to this as the *singular value distribution based discarding* technique and denote the matrix $\mathbf{H}_D$ as the matrix to be inverted once a number of singular values have been discarded.

Before undertaking the experiments described below, a number of further simulations were undertaken in order to establish the feasibility of using the above techniques in practice. This work is described in detail in reference [18]. It was concluded that the GCV technique provided a very useful method for the determination of the Tikhonov regularization parameter and for the determination of the singular values to be discarded. This is also confirmed by the experiments described below.

4. EXPERIMENTS ON THE RECONSTRUCTION OF THE VELOCITY OF A RANDOMLY VIBRATING PLATE

4.1. EXPERIMENTAL APPARATUS

The experiments were performed on a simply supported plate mounted in a finite baffle. Full details of the work are presented in reference [19]. The simply supported boundary condition implies no transverse displacement of the plate edges, although their rotation is permitted. This boundary condition is replicated approximately by the use of shims at the edges of the plate. These are stiff for inplane motion but flexible for rotation. Figure 5 shows the design of the plate. Fifty holes are tapped for 12BA screws with 0·027 m spacing into four edges of an aluminium plate 0·38 m long, 0·3 m wide and 0·0025 m thick. Four shims of $0{\cdot}10 \times 10^{-3}$ mm thick are fabricated into the four edges of the plate through these tapped holes. The aluminium plate and shims fabricated together are fastened to a heavy, very stiff 0·02 m thick steel frame. The inside dimension of the steel frame is 0·38 m long and 0·3 m wide which are precisely the same dimensions as the aluminium plate. Four steel clamping bars 0·01 m thick were used to firmly clamp four shims to the four inside surfaces of the steel frame. The dimensions of the steel frame and clamping were chosen not to produce substructure resonances when the plate is excited. The fabricated simply supported aluminium plate system consisting of plate, shims, steel frame and clamping bars is mounted on a medium density fibreboard (MDF) support box. The simply supported plate system is placed in the centre of a rigid MDF baffle which is 3 m high, 2·8 m wide and 0·012 m thick. In addition, for further reduction of the acoustic interference between the front and rear field of the baffle, an MDF box containing sound absorbent material was made and fastened against the steel main frame via toggle clamps.

The plate was excited by an electromagnetic driver consisting of a coil wound around a core and a permanent magnet. The core of the electromagnetic driver is attached to the rear part of the plate which is not coincident with the nodal lines of many structural modes of interest. This electromagnetic driver generates a force by passing an alternating current through the coil. A random noise signal is used to excite the driver and the force generated is input to the plate. In addition, it was ensured that the mechanical input impedance of the driving system did not exceed the impedance of the plate itself below the frequency of interest. This ensured that the dynamic properties of the plate were not changed.

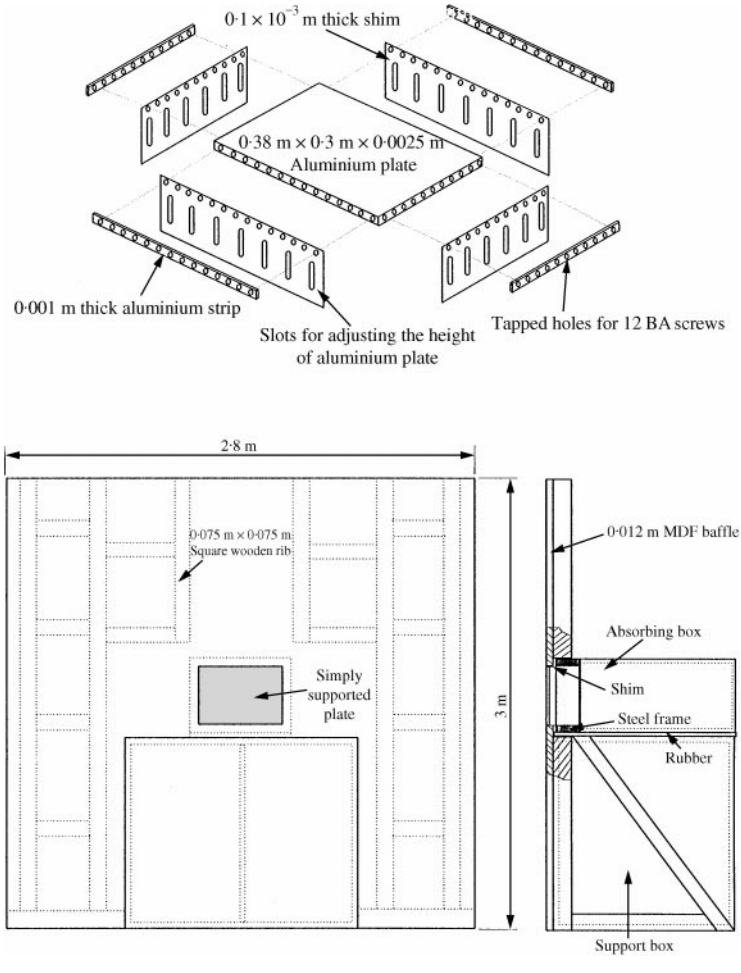

Figure 5. An experimental implementation of a baffled simply supported plate.

The radiated acoustic field is measured by a microphone array supported by a scanning system (see Figure 6) which adjusts the position of the microphone array. The scanner comprises mainly a frame, a stepper motor and a controller, and operates as follows. Six electret microphones are held on the microphone grippers fixed on the vertical aluminium rods which are designed to enlarge the aperture size of the scanning area. The microphone array locates automatically in the horizontal direction by a stepper motor attached to the 0·09 m thick aluminium frame whose dimension is of 1·09 m × 1·39 m × 0·8 m, and manually in the vertical direction by screwing and unscrewing the vertical rods to the aluminium frame. The stepper motor is controlled by the driver which is operated by the control card in connection with the control software, Motion Architect [20] installed in the personal computer. In acquiring pressures by a microphone array and surface velocities by an accelerometer, the current of the coil was also simultaneously obtained to measure the force input by the driving system into the plate. The input force data were used as a normalizer for the pressures and volume velocities. That is to say, the transfer function between the input force and pressures and volume velocities were obtained, instead of pressures and volume velocities themselves. The input force was measured using a force transducer. This,

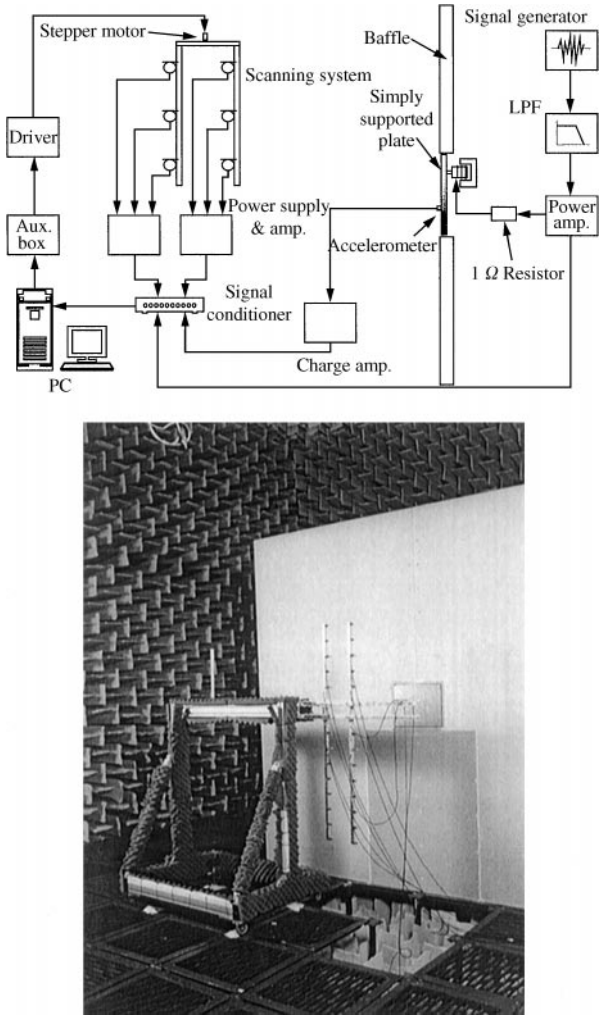

Figure 6. A schematic diagram and a photograph of the experimental set-up.

however, caused a problem of significant mechanical input impedance due to its mass (0·02 kg) when compared to the impedance of the plate itself. To resolve this difficulty, a 1 Ω resistor was connected with the coil cable in series and the voltage between two ends of the resistor is measured. This voltage was therefore proportional to the current flowing in the coil.

In order to evaluate how well the plate replicates the simply supported boundary condition, the modal parameters such as natural frequencies, mode shapes and damping ratios were extracted via a modal test. This was undertaken by the use of a small accelerometer and an impact hammer. The experimental natural frequencies can be compared with the theoretical values which are given in reference [21]. Figure 7 compares the experimental and theoretical natural frequencies which were found to be in good agreement. Also the mode shapes obtained experimentally were compared with those given theoretically [21] and showed reasonably good agreement. The plate can thus be assumed to give a satisfactory replication of the simply supported boundary condition.

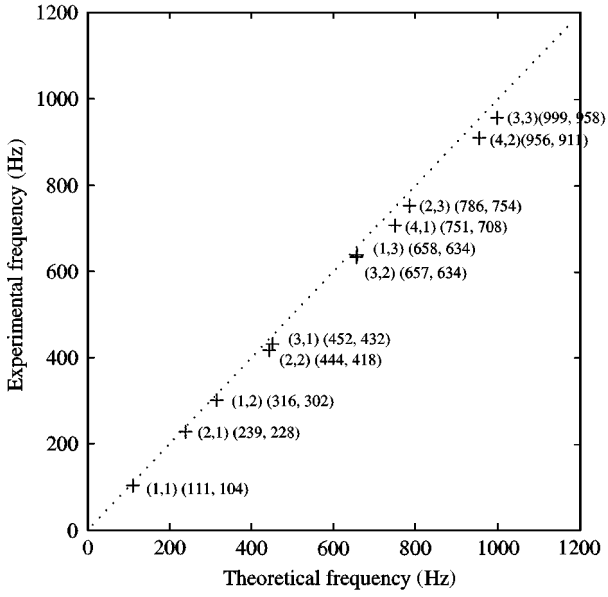

Figure 7. A comparison of the theoretical and experimental natural frequencies of the simply supported plate. Figures in the first parentheses denote the modal indices, and those in the second parentheses the theoretical and experimental natural frequencies respectively.

4.2. DIRECT MEASUREMENT OF THE VOLUME VELOCITY OF THE VIBRATING PLATE

To check how successfully the inverse technique reconstructs volume velocities of a vibrating plate, we need data for comparison and these are obtained from direct measurement. Thus, the direct measurement of volume velocity has to be made as accurately as possible. A number of techniques can be employed for measurement of the volume velocity including an accelerometer, a laser doppler velocimeter [22] or more recently a volume velocity transducer [23]. Here we used the accelerometer.

If a plate vibrates as like a rigid piston moving in phase, volume velocity q is determined by the expression

$$q = Sv_s. \tag{37}$$

where v_s is the local surface velocity measured at any point on the plate and S is the plate area. However, since the plate does not usually show a rigid piston-like motion, the plate should be discretized into a number of small segments. Each segment is regarded as a rigid piston moving in phase. The total volume velocity in this case is determined by the summation of individual contributions of all segments and thus

$$q = \sum_{i=1}^{K} S_i v_{si}, \tag{38}$$

where v_{si} and S_i are the volume velocity and area of the ith segment and K is the total number of segments. It is straightforward to measure the volume velocities by use of the accelerometer. However, a major shortcoming is the additional loading due to the accelerometer attached to the plate, which can cause a change of the dynamic behaviour of

the plate. For this reason, it was necessary to use an accelerometer that was as small as possible. A comparison of the plate impedance and that of the point mass associated with the accelerometer revealed that results should be reliable up to a frequency of around 1700 Hz [19]. In addition, in order to obtain the volume velocity at high frequencies as accurately as possible, the number of measurement points should be sufficient to avoid spatial aliasing.

The plate is thus divided into 144 (12×12) contiguous small rectangular segments of the same area. Measurements of the surface velocities are then made at the individual centre points of these segments. The volume velocity source consists of the combination of some rectangular segments and then its strength is obtained by the summation of the surface velocities of individual segments multiplied by the area of segment. The measurement of the surface velocities is made by a calibrated accelerometer, which is in turn moved to the centre points of the 144 small rectangular elements. The results of the directly measured volume velocities will be presented in the ensuring sections, where these are compared with those estimated by the inverse techniques.

5. EXPERIMENTAL RESULTS

5.1. EXPERIMENTAL RECONSTRUCTION BY THE LEAST-SQUARES METHOD

All experiments have been undertaken in the anechoic chamber (which is of dimensions $9{\cdot}15\text{ m} \times 9{\cdot}15\text{ m} \times 7{\cdot}32\text{ m}$) of the ISVR at the University of Southampton. Since the condition number of the matrix to be inverted plays a crucial role, experiments are conducted for the two main groups which have "small" or "large" condition number (although, strictly speaking, there is not an explicit quantitative scale to distinguish between small and large condition numbers). With the first group, we wish to explore how accurately the simple least-squares solution is able to reconstruct volume velocity sources of the randomly vibrating plate. The second group of experiments are used to investigate how Tikhonov regularization and singular value discarding improve the reconstruction accuracy.

In this section, we present the results of the first group of experiments. An initial experiment is carried out for the system as shown in Figure 8. The plate is discretized into four volume velocity sources each of which consists of 36 (6×6) of 144 small segments. Four microphones are placed symmetrically with respect to the sources, setting the microphone-to-microphone distance equal to the source-to-source distance (0·19 m in the horizontal direction and 0·15 m in the vertical direction). Also the pattern of microphone array is rectangular and the same as that of source array. This geometrical arrangement is selected to make the condition number as small as possible, referring to the behaviour of the condition number of $\mathbf{H}^{\mathrm{H}}\mathbf{H}$ described in reference [1]. The condition number for this case is shown in Figure 9 and is between 50–300, decreasing as frequency increases. In the experiment using this model, the frequency to be analyzed is limited to 500 Hz. This is because the discretized individual rectangular elements are regarded as equivalent point monopole sources and therefore the requirement of the condition $ka \ll 1$ has to be met (a is the typical dimension of a source element, here $a = L_x/4 = 0{\cdot}38/4 = 0{\cdot}095$ m and $k = \omega/c_0$ is the wavenumber of sound in air at the frequency ω). Some of the reconstructed magnitudes and phases of acoustic source strength auto- and cross-spectra are presented in Figure 10. They are in very good agreement with the directly measured values.

The next experiment was conducted for the plate model discretized into 16 volume velocity sources as shown in Figure 11. Each volume velocity source of this model is clearly

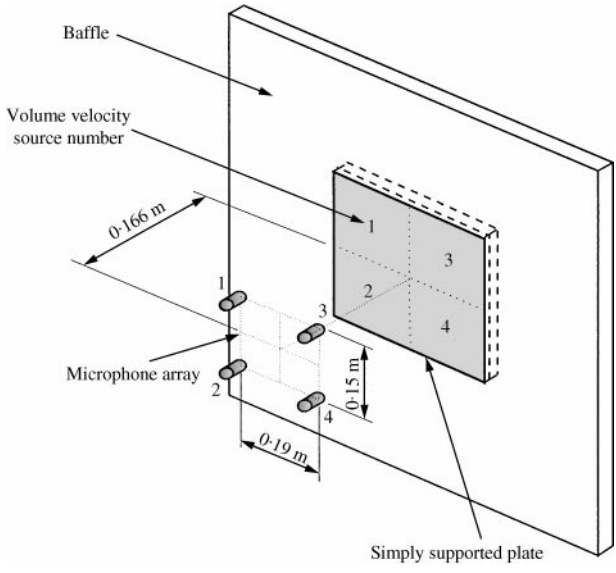

Figure 8. A geometrical arrangement of the plate system discretized into four volume velocity sources and four microphones.

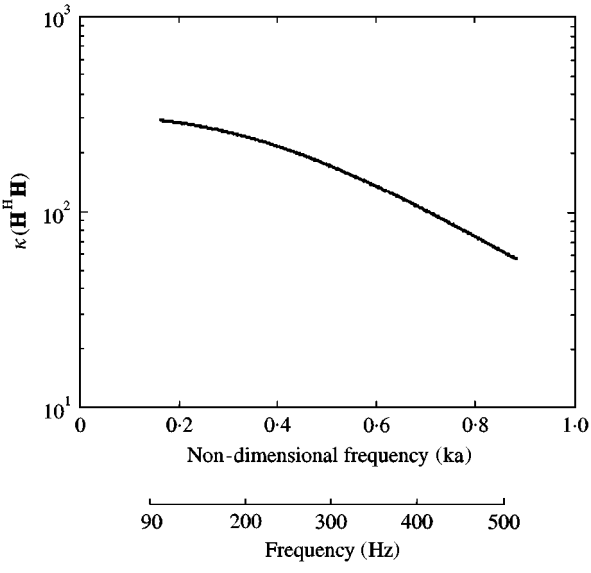

Figure 9. Condition number $\kappa(\mathbf{H}^H\mathbf{H})$ of the model of Figure 8.

smaller than that of the preceding experimental model. In this case, the frequency to be analyzed can be expanded to 1000 Hz, based on $ka \ll 1$ (here $a = L_x/8 = 0{\cdot}38/8 = 0{\cdot}0475$ m). Since the source-to-source distance becomes smaller (i.e., 0·095 m in the horizontal direction and 0·075 m in the vertical direction). Additionally, the 16 microphone array plane is put close to the source array plane at distance of 0·046 m (and, of course, the microphone array is placed symmetrically with respect to the source array). Such a placement makes the

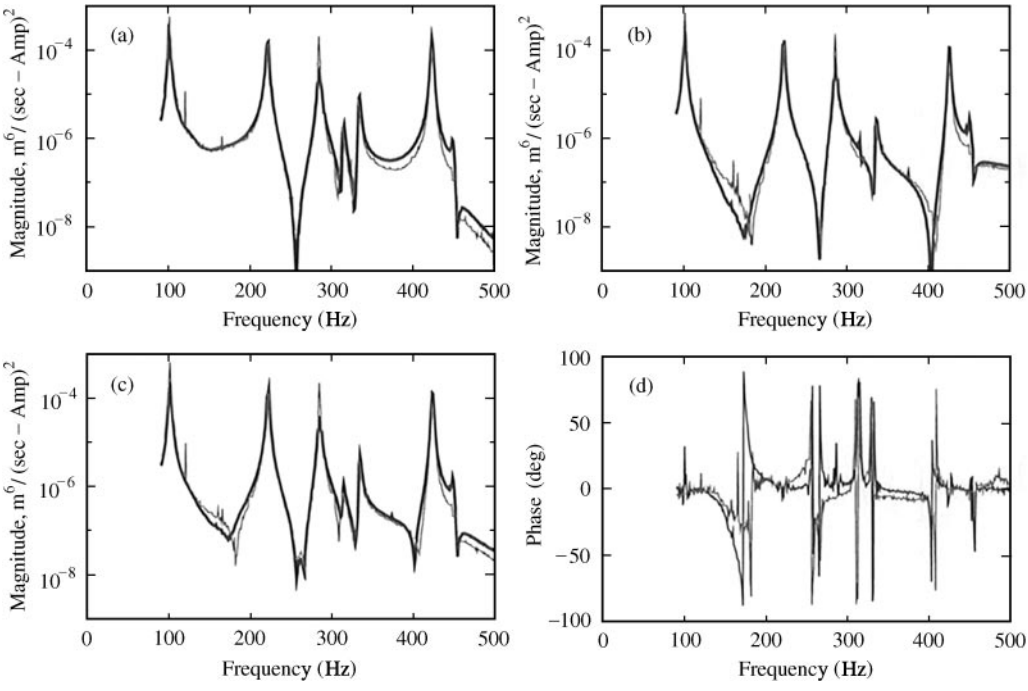

Figure 10. A comparison of the directly measured (black) and reconstructed (by the least-squares solution, grey) volume velocity (per unit ampere) auto-spectra of sources (a) 2, (b) 3 and cross-spectra between sources 2 and 3 ((c) magnitude, (d) phase) for the model of Figure 8.

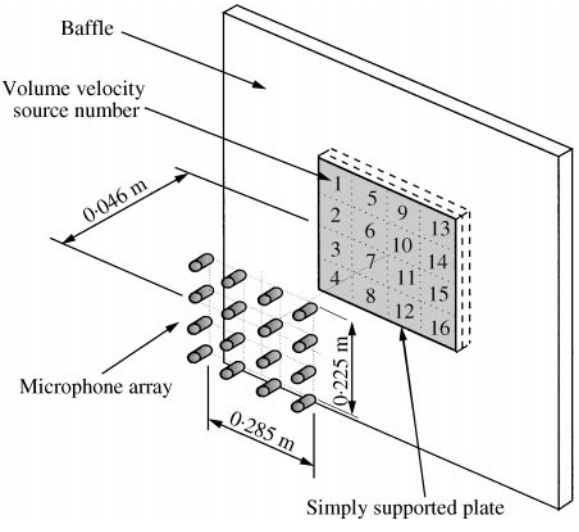

Figure 11. A geometrical arrangement of the plate system discretized into 16 volume velocity sources and 16 microphones.

condition number below 300 (see Figure 12). Note that this condition number is very similar to that of the model of Figure 8 (four sources and four microphones) in spite of the use of more sources and microphones. The results of Figure 13 compare the reconstructed and directly measured volume velocities for this experimental model. The reconstructed values

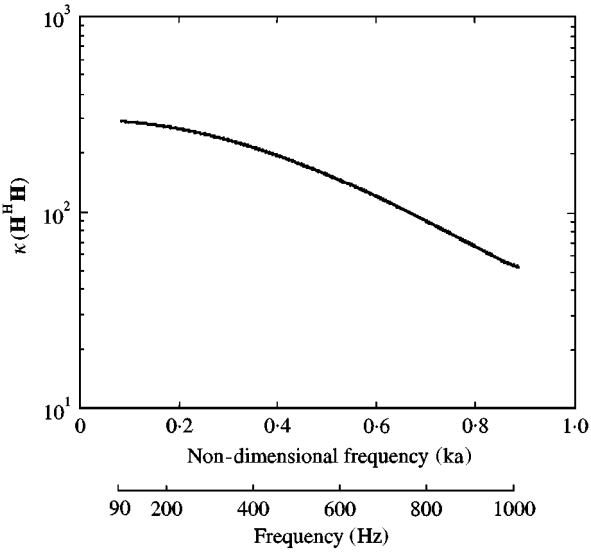

Figure 12. Condition number $\kappa(\mathbf{H}^H\mathbf{H})$ of the model of Figure 11.

follow well the overall trend of the values measured directly up to 1000 Hz. However, the results show a more noisy shape than previously (compare Figure 13 with Figure 10). This is, as expected caused by acoustical reflection from the microphone scanner put close to the plate. Note that the magnitudes of acoustic source strength become smaller than those of the case of the plate discretized into 4 volume velocity sources. The reason for this is that the volume velocity of one source is obtained from the summation of surface velocities multiplied by the area of the rectangular segments enclosed by the boundary of each volume velocity source. Although the results are not shown here, a satisfactory reconstruction was achieved [19] from another experiment using the plate discretized into six volume velocities with the six appropriately placed microphones to produce a well-conditioned matrix to be inverted.

The foregoing experiments are for the models in which the matrix $\mathbf{H}^H\mathbf{H}$ to be inverted is well-conditioned. What if the conditioning becomes poor? Let us first consider the experimental model depicted in Figure 14. Although this consists of four volume velocity sources and four microphones, the condition number presented in Figure 15 is much larger (i.e., 7×10^2–6×10^4) than that of Figure 9 which also comprises four volume velocity sources and four microphones. What is more, it is much larger than that of the 16 volume velocity source and 16 microphone model (Figure 12). The consequence of this poor conditioning is a noisy and erroneous reconstruction, as can be seen from Figure 16. In particular, a noticeable discrepancy appears below about 270 Hz in the magnitude plots. This is caused by the relatively large condition number at these frequencies compared to that at other frequencies where the overall trend of the inverse reconstruction follows well the directly measured results. Also the phases are reconstructed with deteriorated accuracy.

The next experiment was performed using six microphones instead of four microphones for the same plate discretization as illustrated in Figure 17. Moreover, the microphone array is moved further from the plate (to 1·02 m). This enables an investigation of the effect of the worsened conditioning produced by the increase of the source array

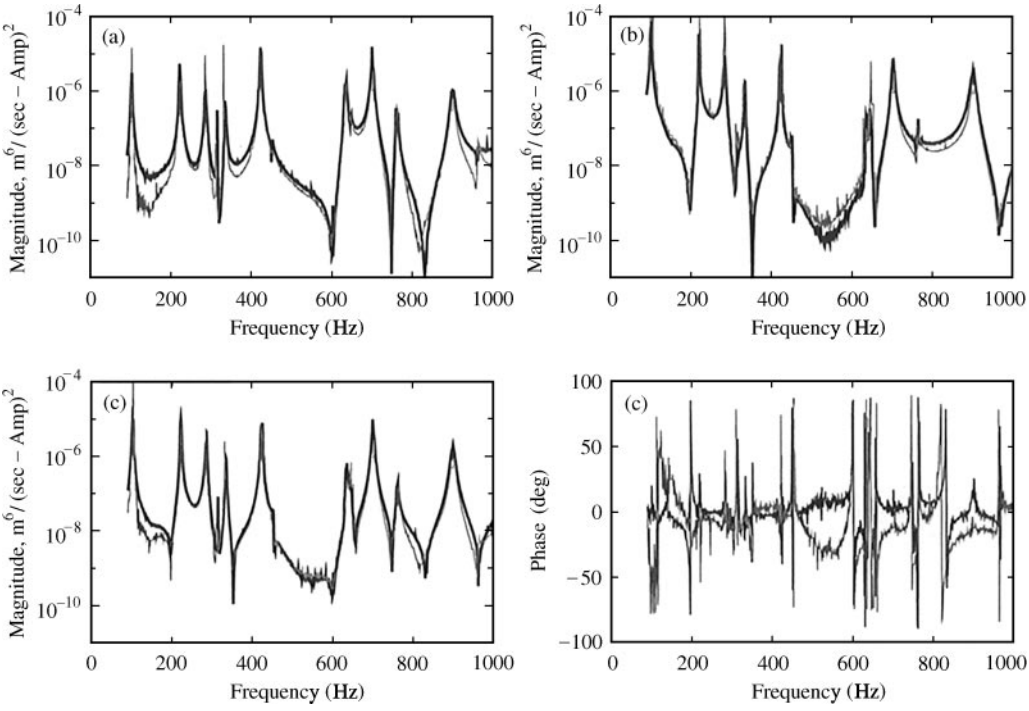

Figure 13. A comparison of the directly measured (black) and reconstructed (by the simple least-squares solution, grey) volume velocity (per unit ampere) auto-spectra of sources (a) 1, (b) 11 and cross-spectra between sources 1 and 11 ((c) magnitude, (d) phase) for the model of Figure 11.

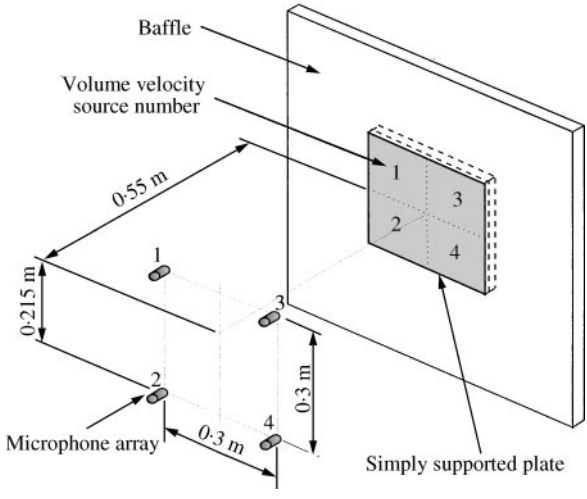

Figure 14. A geometrical arrangement of the plate system discretized into four volume velocity sources and four microphones.

plane-to-microphone array plane distance. The condition number for this case can be observed from Figure 18 and it is between 3×10^3 and 8×10^5. As a result of the enlarged condition number, the magnitudes and phases of restored acoustic source strength deviate significantly from the directly measured values (Figure 19).

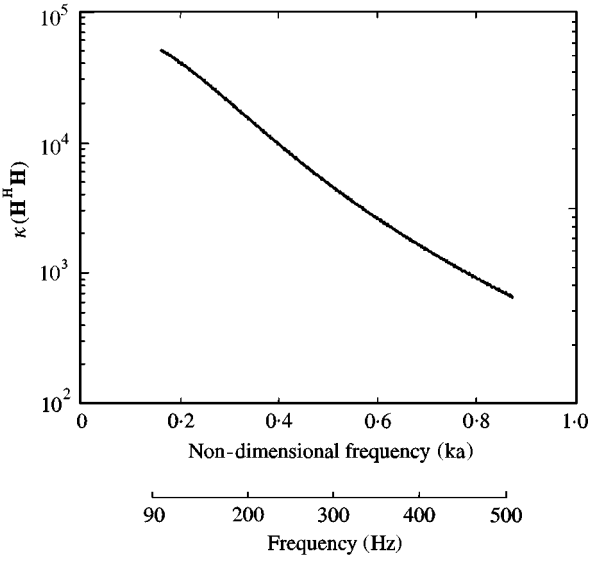

Figure 15. Condition number $\kappa(\mathbf{H}^H\mathbf{H})$ of the model of Figure 14.

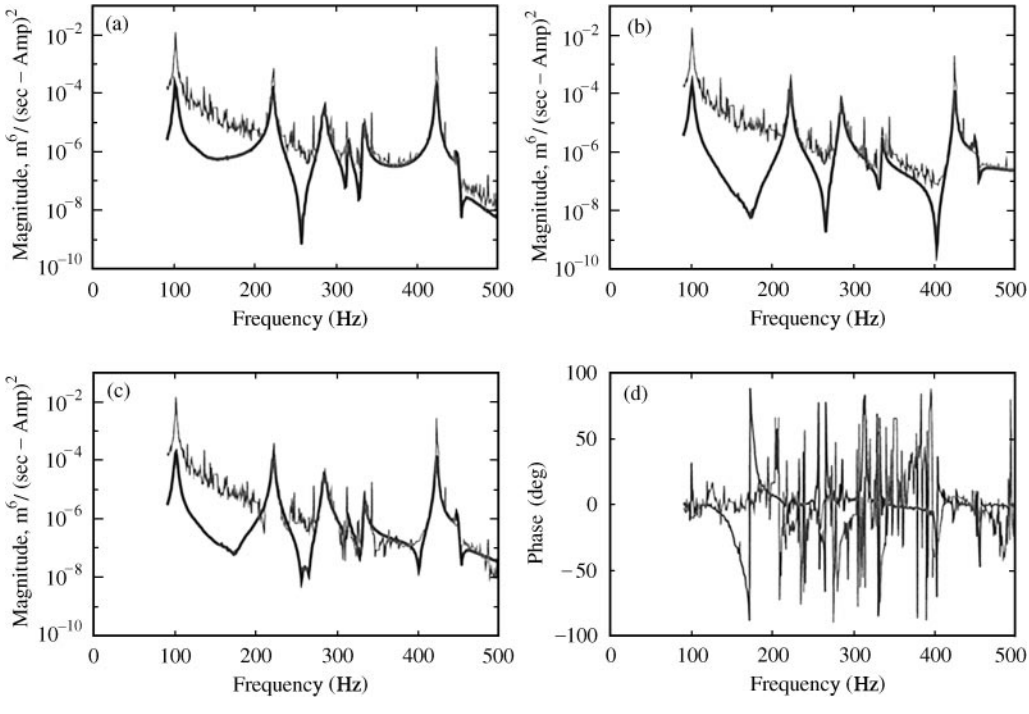

Figure 16. A comparison of the directly measured (black) and reconstructed (by the least-squares solution, grey) volume velocity (per unit ampere) auto-spectra of sources (a) 2, (b) 3 and cross-spectra between sources 2 and 3 ((c) magnitude, (d) phase) for the model of Figure 14.

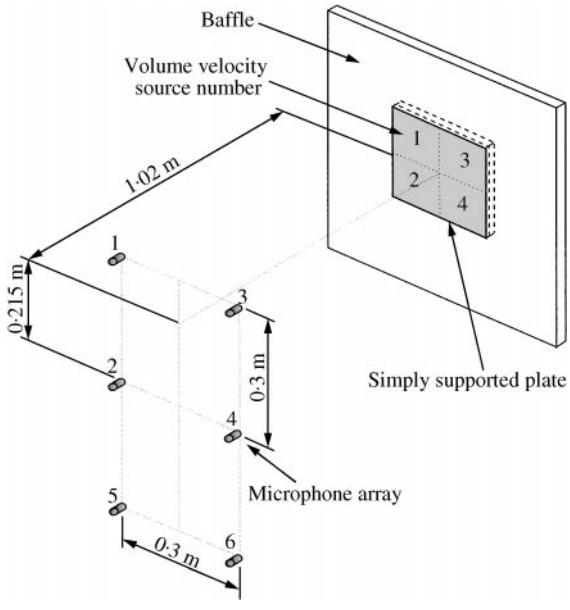

Figure 17. A geometrical arrangement of the plate system discretized into four volume velocity sources and six microphones.

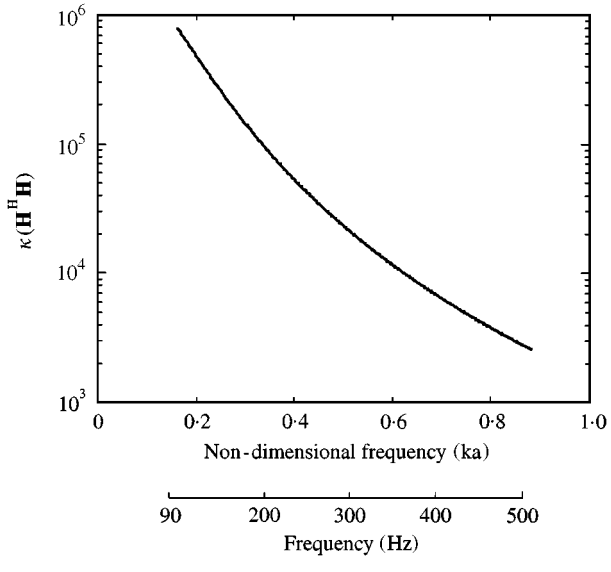

Figure 18. Condition number $\kappa(\mathbf{H}^H\mathbf{H})$ of the model of Figure 17.

Now let us reconsider the experimental model comprising 16 volume velocity sources and 16 microphones. As can be seen from Figure 20, we now enlarge the microphone-to-microphone horizontal and vertical distances to 0·2 m from 0·075 and 0·095 m (Figure 11) and the source array plane-to-microphone array plane distance to 0·661 m from 0·046 m, but leaving the geometry of microphone array symmetric with respect to the volume velocity source array. Such a positioning of microphones is directed towards increasing the

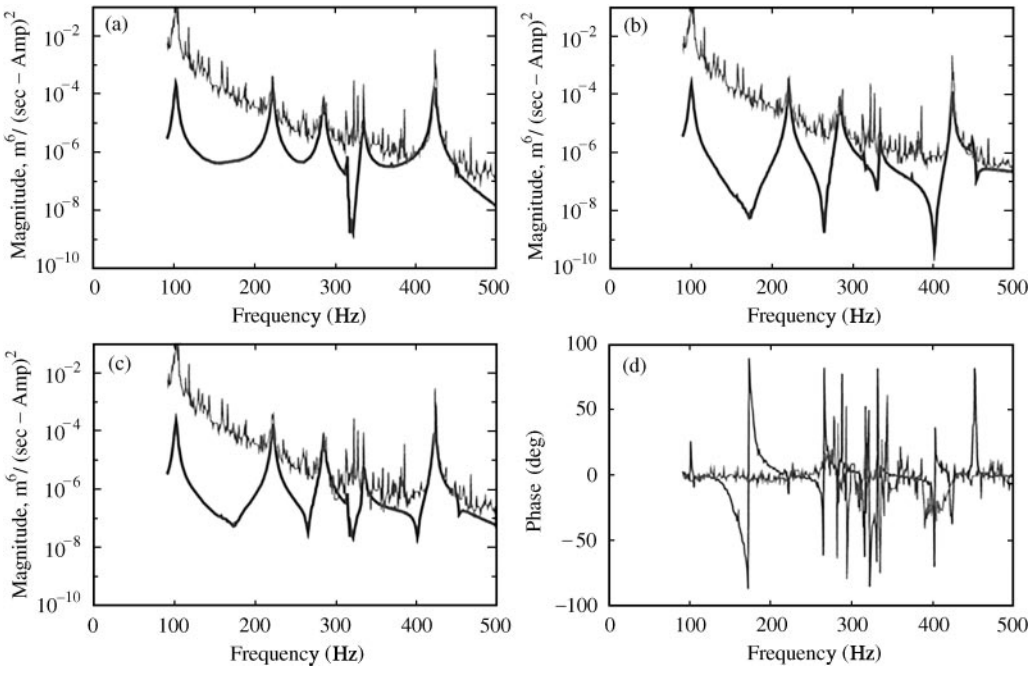

Figure 19. A comparison of the directly measured (black) and reconstructed (by the least-squares solution, grey) volume velocity (per unit ampere) auto-spectra of sources (a) 1, (b) 3 and cross-spectra between sources 1 and 3 ((c) magnitude, (d) phase) for the model of Figure 17.

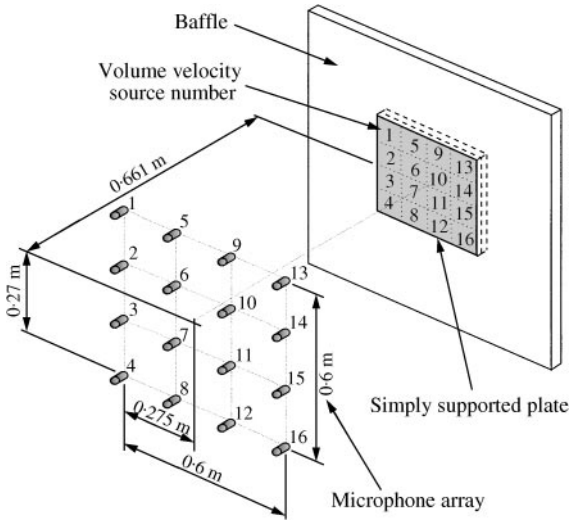

Figure 20. A geometrical arrangement of the plate system discretized into 16 volume velocity sources and 16 microphones.

condition number, i.e., 6×10^6–$1{\cdot}5 \times 10^9$, as plotted in Figure 21. This is because the ratio of the microphone-to-microphone distance to the source-to-source distance is not close to unity (say, $0{\cdot}2/(0{\cdot}3/4) = 2{\cdot}7$ and $0{\cdot}2/(0{\cdot}38/4) = 2{\cdot}1$ in the vertical and horizontal direction, respectively), and furthermore the microphone array is positioned far from the plate

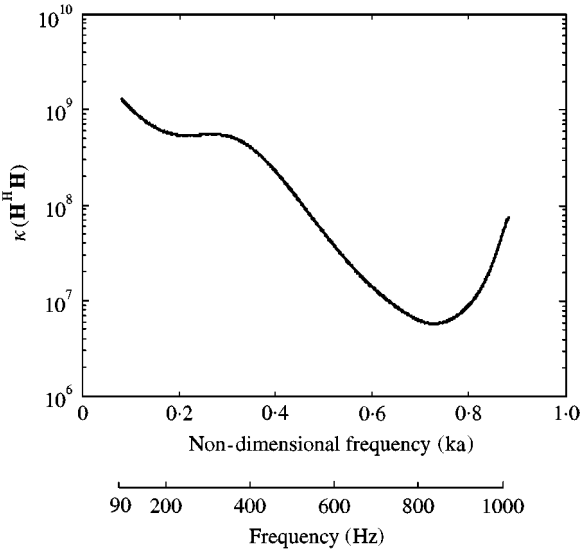

Figure 21. Condition number $\kappa(\mathbf{H}^{\mathrm{H}}\mathbf{H})$ of the model of Figure 20.

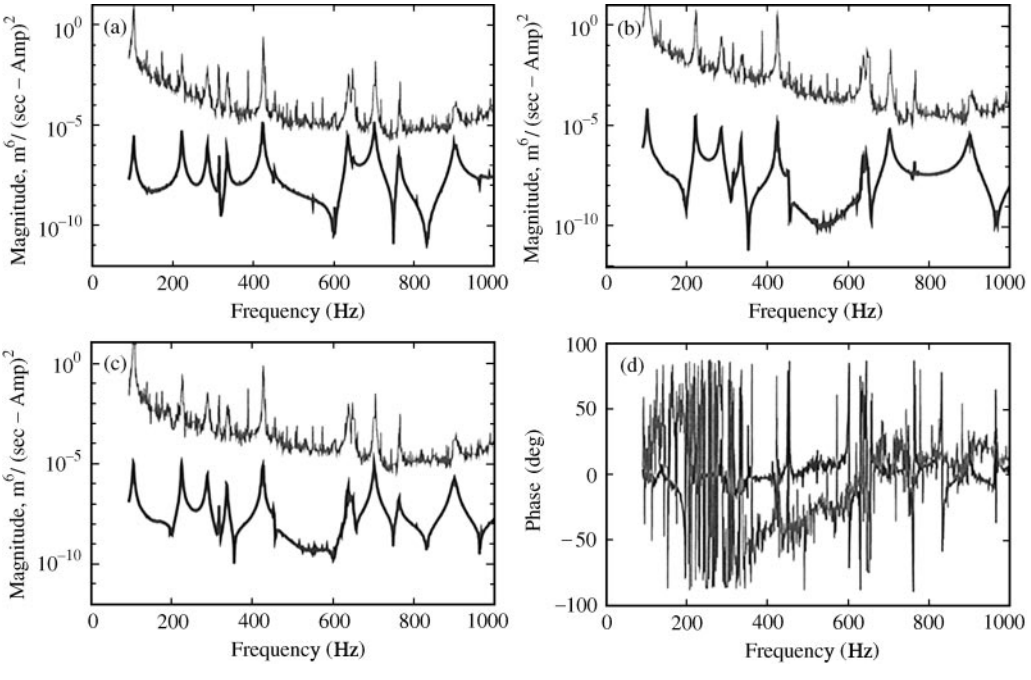

Figure 22. A comparison of the directly measured (black) and reconstructed (by the simple least-squares solution, grey) volume velocity (per unit ampere) auto-spectra of sources (a) 1, (b) 11 and cross-spectra between sources 1 and 11 ((c) magnitude, (d) phase) for the model of Figure 20.

compared to the source-to-source distance. With this poor conditioning, the simple least-squares approach cannot help but restore acoustic source strength very inaccurately. From the overall point of view, as plotted in Figure 22, the reconstructed magnitudes reveal a biased pattern from the directly measured values, even though the peaks at resonant

frequencies can be seen. The restored phases also are in substantial disagreement with the directly measured values.

As observed from the above results, it is easily recognized that the essence of the successful reconstruction of acoustic source strength by the simple least-squares method lies on keeping the condition number as small as possible by adjusting the geometrical arrangement of discretized sources and microphones, as long as the experimental environment is sufficient to suppress the strong effect of noise. Also, even though it is not straightforward to express quantitatively the boundary of the large and small condition numbers, a rough guide can be extracted for the case examined here. The above results suggest that if the condition number of the matrix $\mathbf{H}^{\mathrm{H}}\mathbf{H}$ to be inverted is below about 10^3, then the least-squares method can provide a satisfactory reconstruction, without using regularization methods.

5.2. EXPERIMENTAL RECONSTRUCTION BY TIKHONOV REGULARIZATION

Here we discuss how Tikhonov regularization improves the accuracy of acoustic source strength of the models (Figures 17 and 20) reconstructed poorly by the least-squares method alone. For the regularization parameters, we use β_{qq} which is found by minimizing the residual $\|\mathbf{S}_{qq} - \mathbf{S}_{qqR}\|_e$ between the desired solution $\mathbf{S}_{qq}$ and the Tikhonov regularized solution $\mathbf{S}_{qqR}$, and β_{GCV} which is the minimizer of the generalized cross-validation function $V(\beta)$. Although the regularization parameter β_{qq} can be chosen only when having prior knowledge of either the volume velocity or the noise, this is used here as a comparator to check the performance of β_{GCV} which is determined without such prior knowledge.

Tikhonov regularization is first applied to the experimental model consisting of 4 discretized sources and 6 microphones illustrated in Figure 17. In this case the least-squares approach could not produce a satisfactory reconstruction (Figure 19). For this model, we designed the regularization parameters β_{qq} and β_{GCV} by following the procedure given by Figures 3 and 4 respectively. The result of Figure 23 compares the two

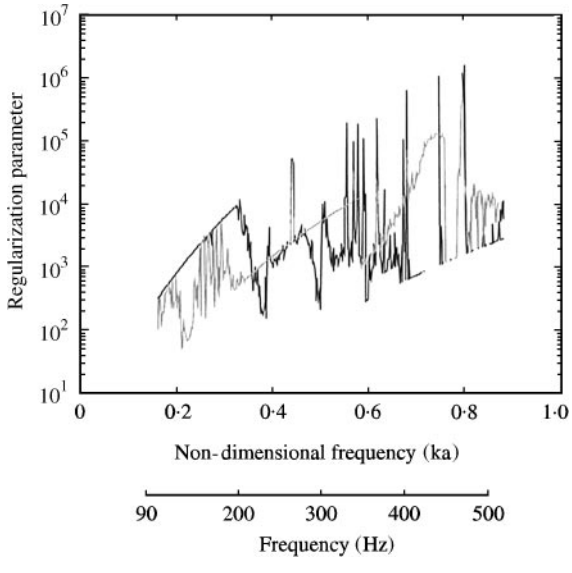

Figure 23. Regularization parameters for the model of Figure 17: β_{qq} (black) and β_{GCV} (grey). $a = L_x/4$, $L_x = 0{\cdot}38$ m.

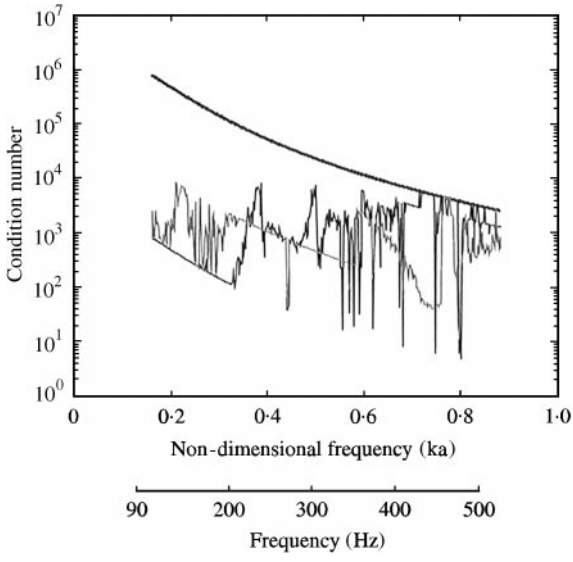

Figure 24. Condition numbers for the model of Figure 17: $\kappa(\mathbf{H}^{\mathrm{H}}\mathbf{H})$ (thick black), $\kappa(\mathbf{H}^{\mathrm{H}}\mathbf{H} + \beta_{qq}\mathbf{I})$ (thin black) and $\kappa(\mathbf{H}^{\mathrm{H}}\mathbf{H} + \beta_{GCV}\mathbf{I})$ (grey). $a = L_x/4$, $L_x = 0{\cdot}38$ m.

regularization parameters. They show that the overall trend with frequency is similar to each other, but of course their absolute values are rather different. In this figure, the values at some frequencies (say, about 400–500 Hz) indicate that no regularization is recommended because the volume velocities recovered by the least-squares solution at these frequencies are close to the desired values (see Figure 19). The addition of β_{qq} and β_{GCV} into the diagonal components of the original matrix $\mathbf{H}^{\mathrm{H}}\mathbf{H}$ (see equation (2)) improves the conditioning, as graphed in Figure 24. In particular, at frequencies below about 400 Hz the matrix becomes better conditioned where the least-squares method restored acoustic source strength poorly (see Figure 19). As the result of the improvement of the conditioning from $\kappa(\mathbf{H}^{\mathrm{H}}\mathbf{H})$ to $\kappa(\mathbf{H}^{\mathrm{H}}\mathbf{H} + \beta_{qq}\mathbf{I})$ or $\kappa(\mathbf{H}^{\mathrm{H}}\mathbf{H} + \beta_{GCV}\mathbf{I})$, the Tikhonov regularized solution expressed by equation (2) enhances the accuracy of reconstruction of the magnitudes of volume velocities, as illustrated in Figure 25. As expected, since the values of β_{qq} and β_{GCV} are also similar, the acoustic source strengths recovered by use of β_{qq} and β_{GCV} are similar. Reflecting on the fact that β_{GCV} is determined without *a priori* knowledge of either the volume velocity or the noise, we can see that the GCV technique is a practical tool to improve the accuracy of reconstruction of volume velocities. However, as can be seen from Figure 25, Tikhonov regularization by use of either β_{qq} or β_{GCV} still produces unsatisfactory reconstruction of the phases of the volume velocity cross-spectra between the discretized sources.

The next application of Tikhonov regularization was performed on the experimental model consisting of the plate discretized into 16 volume velocity sources and 16 microphones as shown in Figure 20. The results shown in Figure 26 compares two regularization parameters β_{qq} and β_{GCV} chosen by following the steps presented in Figures 3 and 4. The overall trend is similar in each case, as observed previously. The use of these parameters reduces the original condition number $\kappa(\mathbf{H}^{\mathrm{H}}\mathbf{H})$ into $\kappa(\mathbf{H}^{\mathrm{H}}\mathbf{H} + \beta_{qq}\mathbf{I})$ and $\kappa(\mathbf{H}^{\mathrm{H}}\mathbf{H} + \beta_{GCV}\mathbf{I})$ (approximately 10^{-5} times), as illustrated in Figure 27. The condition numbers of the regularized matrices to be inverted are below 10^4 up to about 500 Hz and below 10^3 beyond this frequency. Recall that for the experimental model having the

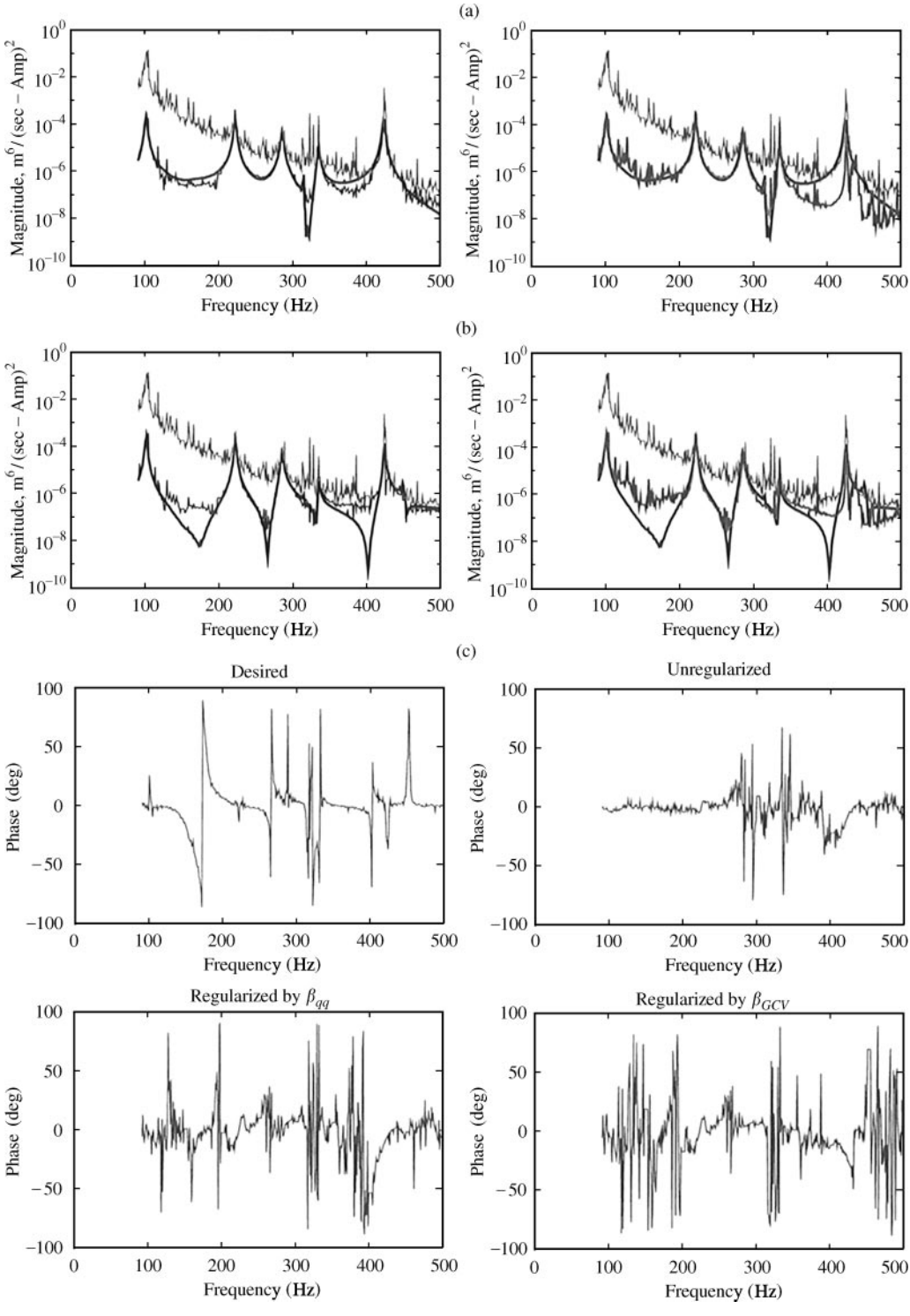

Figure 25. Volume velocity (per unit ampere) auto-spectra of sources (a) 1, (b) 3: desired (thick black), unregularized (thin grey), regularized by β_{qq} (thin black), regularised by β_{GCV} (thick grey). (c) Phase of cross-spectra between sources 1 and 3 for the model of Figure 17.

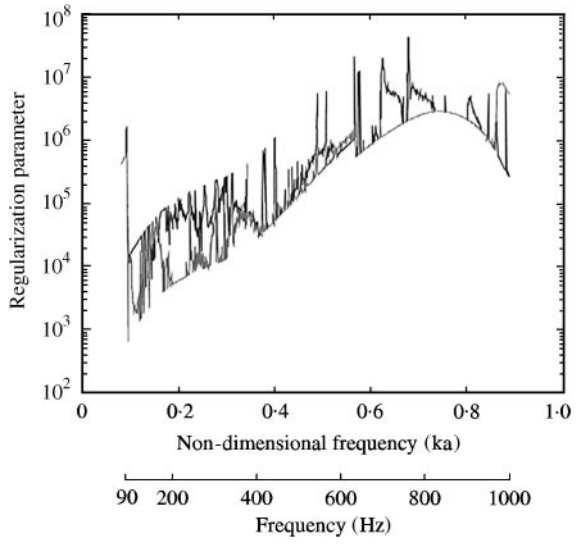

Figure 26. Regularization parameters for the model of Figure 20: β_{qq} (black) and β_{GCV} (grey). $a = L_x/8$, $L_x = 0{\cdot}38$ m.

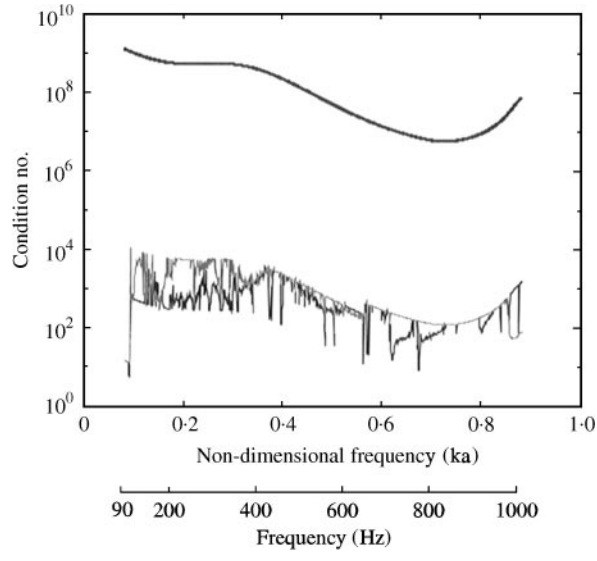

Figure 27. Condition numbers for the model of Figure 20: $\kappa(\mathbf{H}^{\mathrm{H}}\mathbf{H})$ (thick black), $\kappa(\mathbf{H}^{\mathrm{H}}\mathbf{H} + \beta_{qq}\mathbf{I})$ (thin black) and $\kappa(\mathbf{H}^{\mathrm{H}}\mathbf{H} + \beta_{GCV}\mathbf{I})$ (grey). $a = L_x/8$, $L_x = 0{\cdot}38$ m.

condition number below 10^3, the least-squares solution produced a satisfactory reconstruction (see Figures 8–13). With the conditioning improved, the influence of the noise is diminished so effectively that Tikhonov regularized solution using β_{qq} or β_{GCV} reconstructs very remarkably the magnitudes of volume velocities (Figure 28). Note that the magnitudes of volume velocities restored by β_{GCV} are very akin to those recovered by β_{qq}. However, the phase reconstruction is again unsatisfactory.

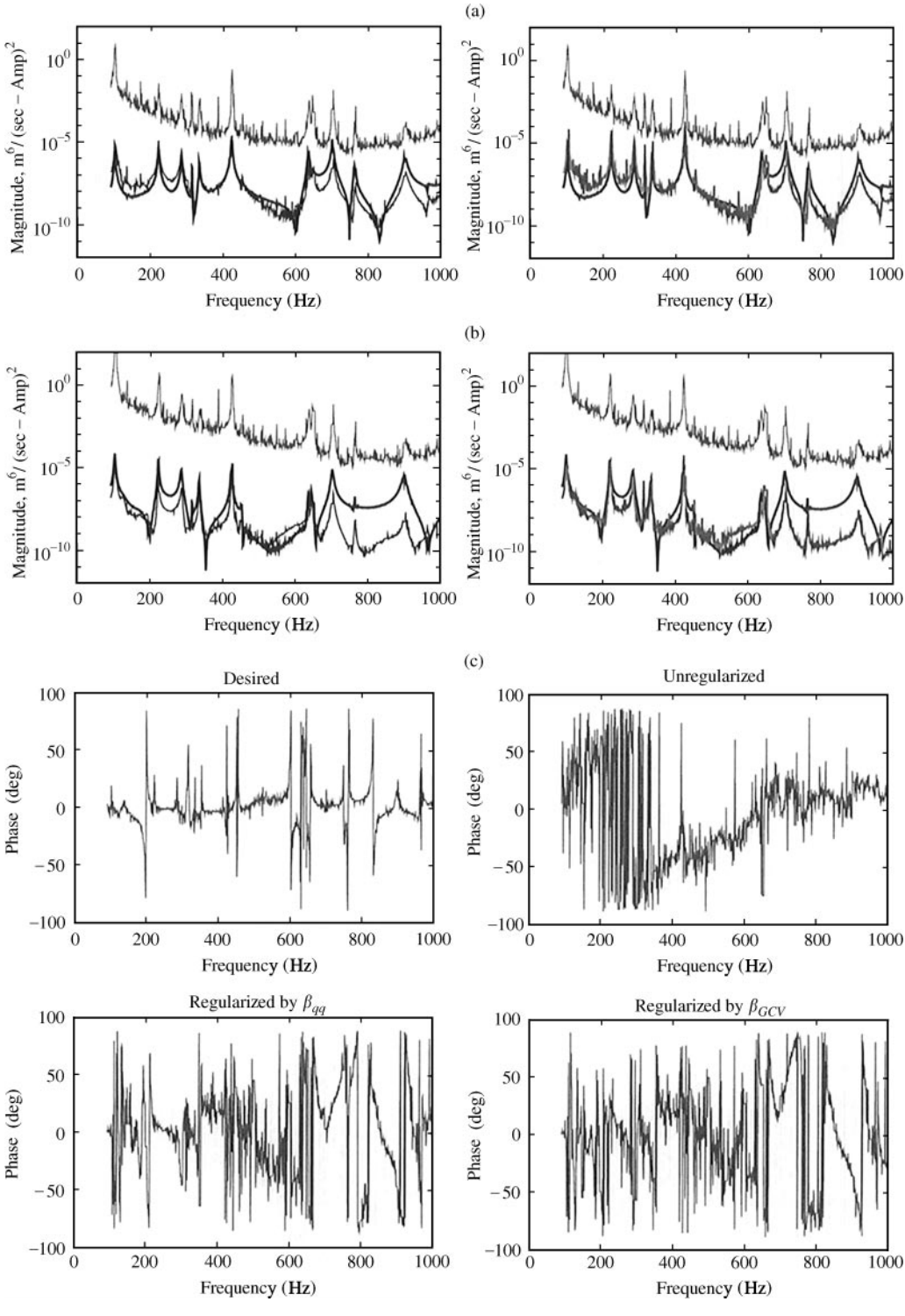

Figure 28. Volume velocity (per unit ampere) auto-spectra of sources (a) 1, (b) 11: desired (thick black), unregularized (thin grey), regularized by β_{qq} (thin black), regularized by β_{GCV} (thick grey). (c) Phase of cross-spectra between sources 1 and 11 for the model of Figure 20.

5.3. EXPERIMENTAL RECONSTRUCTION BY SINGULAR VALUE DISCARDING

Singular value discarding is now performed for the experimental models to which Tikhonov regularization has been applied in the previous section. The first application is used with the model of Figure 17 in which the plate is discretized into four sources and six microphones are employed. Shown in Figure 29 are the singular values of the transfer function matrix $\mathbf{H}$ to be inverted. Their distribution with frequency shows clearly why the conditioning of this model is poor at low frequencies (see Figure 18). Note that the dimensions of $\mathbf{H}$ for this model are 6-by-4 and thus there are four singular values. In order to improve the conditioning, we discard some singular values by either the singular value distribution based discarding technique or the generalized cross-validation technique as discussed in section 3. At first, from the singular value distribution presented in Figure 29, the last singular value is removed for frequencies below 400 Hz. As a result, the conditioning of the matrix to be inverted is improved from $\kappa(\mathbf{H})$ to $\kappa(\mathbf{H}_D)$ as illustrated in Figure 30. In this figure, the overlapping of two lines of $\kappa(\mathbf{H})$ and $\kappa(\mathbf{H}_D)$ beyond 400 Hz indicates no change of conditioning because no singular value was discarded. Another elimination of some singular values is made by using the generalized cross-validation function V_v defined in section 3. Of the calculated values of the V_v function, we select the minimum value. At this point, if the associated $\mathbf{I}_v$ producing the minimum V_v has v unities from the first to the vth element on its diagonal, then the $(v+1)$th to four singular values of the matrix $\mathbf{H}$ (m-by-n, $m \geqslant n$) are truncated. Thus, the matrix $\mathbf{H}$ is transformed into $\mathbf{H}_v$. This is repeated at each component of frequency to be analyzed. Figure 30 compares $\kappa(\mathbf{H}_v)$ with $\kappa(\mathbf{H}_D)$ and shows that $\kappa(\mathbf{H}_v)$ follows $\kappa(\mathbf{H}_D)$ well, except beyond 400 Hz. In this figure, $\kappa(\mathbf{H}_v) = \kappa(\mathbf{H}_D)$ at many frequencies signifies that the minimum value of V_v at those frequencies is achieved by removing only the last (here the fourth) singular value (because $\kappa(\mathbf{H}_D)$ was obtained after discarding the last singular value up to 400 Hz). The results of Figure 31 show some of the reconstructed volume velocities. The magnitudes of volume velocities recovered by using $\mathbf{H}_D$ and $\mathbf{H}_v$ approach the desired values very closely, compared to those achieved by the simple least-squares method. Furthermore, since the levels of conditioning are similar, these

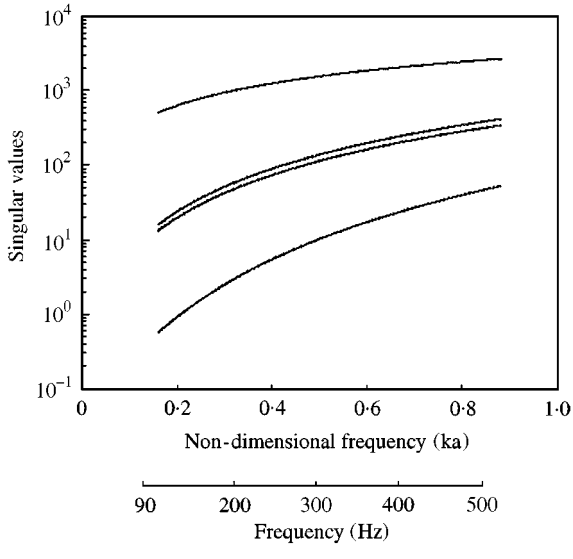

Figure 29. Singular values of the matrix $\mathbf{H}$ for the model of Figure 17. $a = L_x/4$, $L_x = 0{\cdot}38$ m.

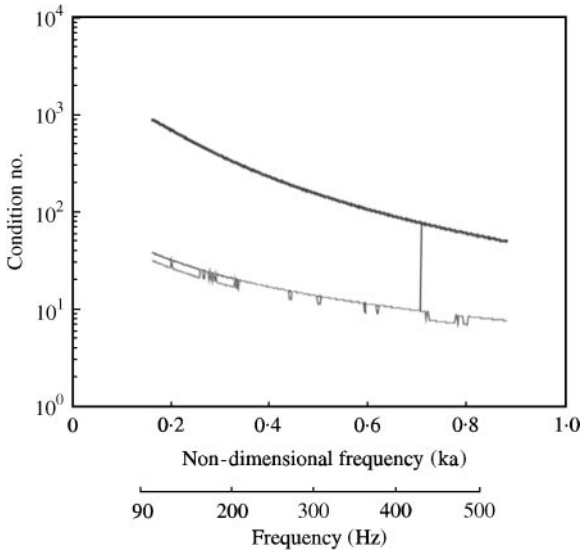

Figure 30. Condition numbers for the model of Figure 17: $\kappa(\mathbf{H})$ (thick black), $\kappa(\mathbf{H}_D)$ (thin black) and $\kappa(\mathbf{H}_v)$ (grey). $a = L_x/4$, $L_x = 0{\cdot}38$ m.

two reconstructed results are similar. In contrast with the magnitude reconstruction, the restored phases again show unsatisfactory results. In the meantime, comparing the results of Figure 31 with Figure 25 reveals that the accuracy of reconstruction by singular value discarding is similar to that given by Tikhonov regularization.

Now we will consider the experimental model given by Figure 20 which consists of the plate discretized into 16 sources and 16 microphones. For this model, a plot of the distribution of 16 singular values is presented in Figure 32. As in the previous case, the choice of singular values to be discarded is made by two methods based on the singular value distribution and generalized cross-validation function. Based on the singular value distribution of Figure 32, we first partition the frequency range of interest, 90–1000 Hz, into three zones: frequencies < 500 Hz, 500 Hz $\leqslant$ frequencies $\leqslant 600$ Hz, and frequencies > 600 Hz. For each zone, the singular values less than 1×10^2, 2×10^2, and 3×10^2 are truncated. Note that these values are chosen arbitrarily based on empirical experience. As a result, the conditioning $\kappa(\mathbf{H})$ of the original matrix $\mathbf{H}$ to be inverted is enhanced by $\kappa(\mathbf{H}_D)$ as plotted in Figure 33. Elimination of some singular values by using generalized cross-validation is performed as in the previous case. However, since the dimension of $\mathbf{I}_v$ of this model is 16-by-16, the calculation of the V_v function is repeated until the third to 16th diagonal components of $\mathbf{I}_v$ are replaced by zero. Plotted in Figure 33 is the condition number of the matrix $\mathbf{H}_v$. Unlike the previous case of Figure 30, $\kappa(\mathbf{H}_v)$ is mostly different from $\kappa(\mathbf{H}_D)$ and shows a noisy pattern. The results of Figure 34 illustrate that the use of the singular value discarded matrix $\mathbf{H}_D$ instead of the original matrix $\mathbf{H}$ improves the accuracy of reconstruction of the magnitudes of volume velocities which were restored badly by the simple least-squares method alone. In contrast with this the use of $\mathbf{H}_v$ reconstructs the magnitudes of volume velocities unsatisfactorily, revealing a noisy shape. Needless to say, this is in connection with $\kappa(\mathbf{H}_v)$ having a noisy pattern, which indicates that for this model singular value discarding by minimizing the generalized cross-validation function does not appear to work satisfactorily. For this model the phase recovery by both $\mathbf{H}_D$ and $\mathbf{H}_v$ is poor.

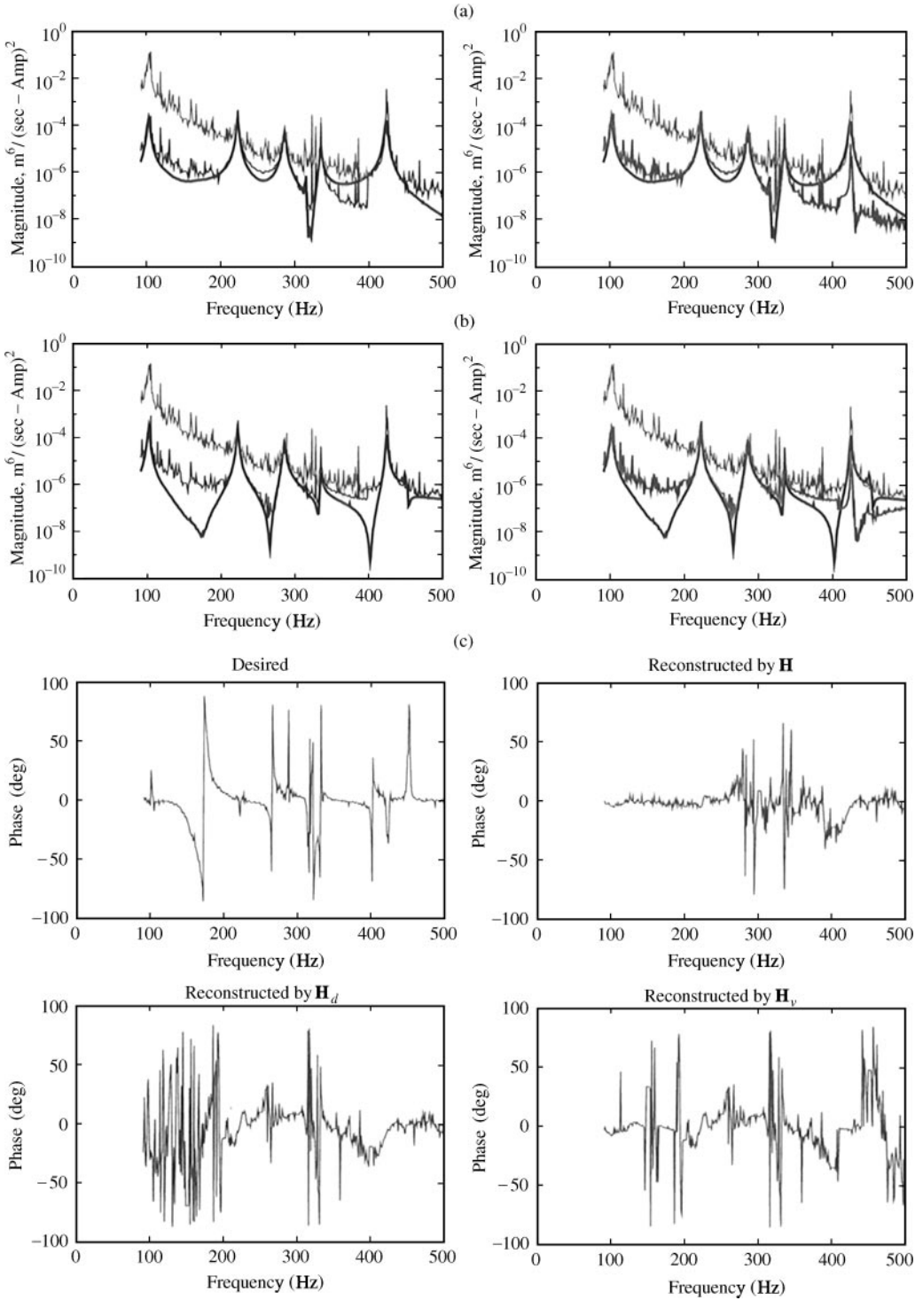

Figure 31. Volume velocity (per unit ampere) auto-spectra of sources (a) 1, (b) 3: desired (thick black), undiscarded (thin grey), reconstructed by $\mathbf{H}_D$ (thin black), reconstructed by $\mathbf{H}_v$ (thick grey). (c) Phase of cross-spectra between sources 1 and 3 for the model of Figure 17.

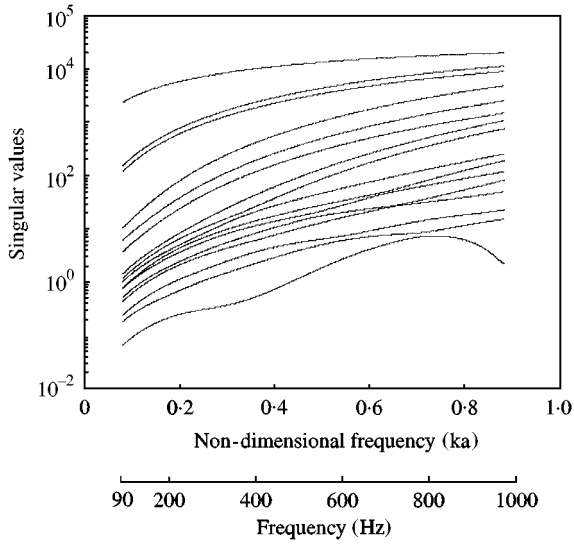

Figure 32. Singular values of the matrix **H** for the model of Figure 20. $a = L_x/8$, $L_x = 0{\cdot}38$ m.

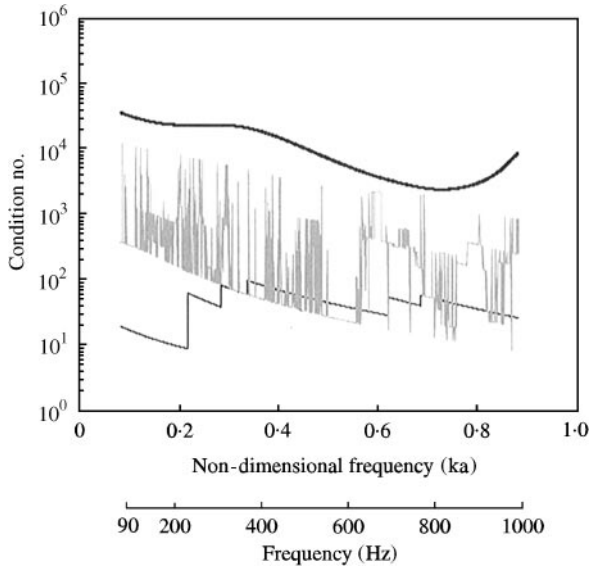

Figure 33. Condition numbers for the model of Figure 20: $\kappa(\mathbf{H})$ (thick black), $\kappa(\mathbf{H}_D)$ (thin black) and $\kappa(\mathbf{H}_v)$ (grey). $a = L_x/8$, $L_x = 0{\cdot}38$ m.

From the experimental reconstruction results presented above, it has been observed that the application of Tikhonov regularization or singular value discarding to an ill-conditioned system can provide considerable improvement in accuracy of reconstruction. Also, the GCV technique has been seen to be a practical tool for choosing properly the regularization parameter and the singular values to be truncated. However, stress should be laid on the fact that the GCV technique does not always lead to a successful choice of those values. As could be seen, the GCV technique has chosen appropriately the regularization

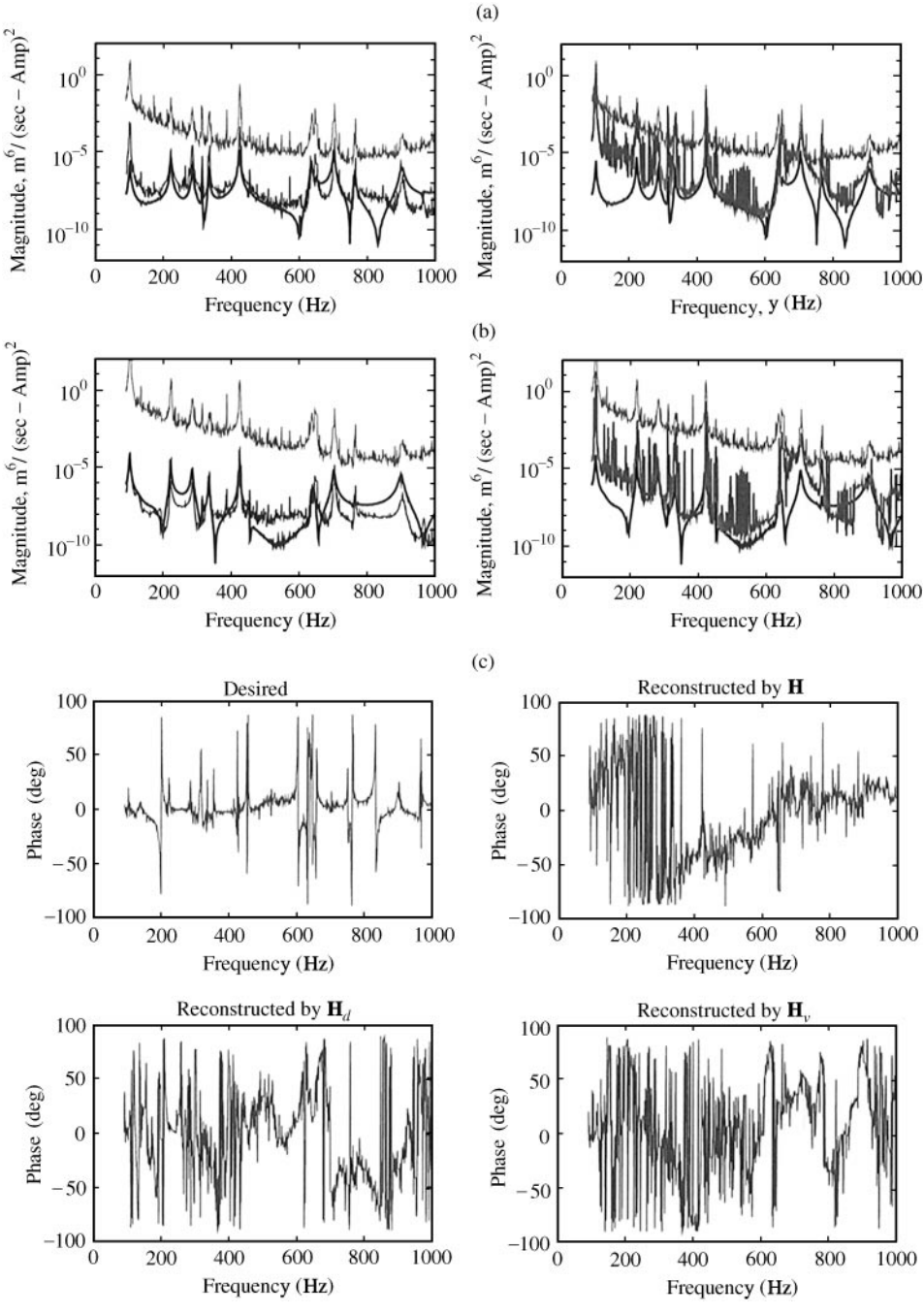

Figure 34. Volume velocity (per unit ampere) auto-spectra of sources (a) 1, (b) 11: desired (thick black), undiscarded (thin grey), reconstructed by $\mathbf{H}_D$ (thin black), reconstructed by $\mathbf{H}_v$ (thick grey). (c) Phase of cross-spectra between sources 1 and 11 for the model of Figure 20.

parameters and the singular values to be eliminated for most of the experimental models considered up to now. However, this had not decided properly the singular values to be eliminated for the 16 source and 16 microphone model. Accordingly, in applying the GCV technique, we have to recall the cautionary remarks referred to section 2.

6. CONCLUSIONS

Through a series of experiments using various models, the least-squares method has been shown to be capable of reconstructing the volume velocities of a randomly vibrating simply supported plate with good accuracy, when the conditioning of the matrix to be inverted is made small. Although it is in general not straightforward to judge the boundary between "small" and "large" condition numbers, the experimental results presented here suggest that the condition number of the matrix $\mathbf{H}^{\mathrm{H}}\mathbf{H}$ can be said to be small when this is below about 10^3. Tikhonov regularization using β_{GCV} which is chosen by minimizing the generalized cross-validation function improves considerably the poor accuracy of volume velocities reconstructed by the least-squares method alone. These results have shown a similar trend to those reconstructed by using β_{qq} which is used as comparator to check the performance of β_{GCV} and is determined by minimizing the difference between the desired and estimated volume velocities. However, the regularization parameters β_{qq} and β_{GCV} have also shown unsatisfactory performance in improving the phases of volume velocity cross-spectra reconstructed poorly by the least-squares method alone. Singular value discarding based on the singular value distribution has shown that the volume velocity distributions and their interactions can be reconstructed more approximately, compared to the values obtained by only the simple least-squares method. On the contrary, singular value discarding using the generalized cross-validation technique has revealed a model-dependent performance. This is thought to be a limitation of the generalized cross-validation technique, which has been already pointed out by some researchers.

ACKNOWLEDGMENT

This research was financially supported by the Daewoo Motor Company, Korea.

REFERENCES

1. P. A. Nelson and S. H. Yoon 1998 *Journal of Sound and Vibration* **233**, 643–668. Estimation of acoustic source strength by inverse methods: Part I, Conditioning of the inverse problem.
2. G. H. Golub, M. Heath and G. Wahba 1979 *Technometrics* **21**, 215–223. Generalized cross-validation as a method for choosing a good ridge parameter.
3. N. P. Galatsanos and A. K. Katsaggelos 1992 *IEEE Transactions on Image Processing* **1**, 322–336. Methods for choosing the regularisation parameter and estimating the noise variance in image restoration and their relation.
4. M. Allen 1974 *Technometrics* **16**, 125–127. The relationship between variable selection and data augmentation and a method for prediction.
5. B. Drachman 1984 *IEEE Transactions on Antennas and Propagation* **AP-32**, 219–225. Two methods to deconvole: L_1-method using simplex algorithm and L_2-method using least squares and a parameter.
6. A. M. Thompson, J. C. Brown, J. W. Kay and M. Titterington 1991 *IEEE Transactions on Pattern Analysis and Machine Intelligence* **13**, 326–339. A study of methods of choosing the smoothing parameter in image restoration by regularisation.
7. P. C. Hansen and D. P. O'Leary 1993 *SIAM Journal on Scientific Computing* **14**, 1487–1503. The use of the L-curve in the regularisation of discrete ill-posed problems.
8. B. Anderssen and P. Bloomfield 1974 *Numerische Mathematik* **22**, 157–182. Numerical differentiation procedures for non-exact data.
9. G. Wahba and S. Wold 1975 *Communications Statistics* **4**, 1–17. A completely automatic French curve: fitting splines by cross validation.
10. P. Craven and G. Wahba 1979. *Numerische Mathematik* **31**, 377–403. Smoothing noisy data with spline functions-estimating the correct degree of smoothing by the method of generalised cross-validation.

11. S. BARNETT 1990 *Matrices: Methods and Applications*. Oxford: Oxford University Press.
12. G. WAHBA 1990 *CBMS-NSF Regional Conference Series in Applied Mathematics* **59**, Philadelphia, PA: Society for Industrial and Applied Mathematics. Spline Models for Observation Data.
13. A. M. THOMPSON, J. W. KAY and M. TITTERINGTON 1989 *Journal of Statistics and Computational Simulation* **33**, 199–216. A cautionary note about crossvalidatory choice.
14. E. ROTHWELL and B. DRACHMAN 1989 *International Journal for Numerical Methods in Engineering* **28**, 609–620. A unified approach to solving ill-conditioned matrix problems.
15. R. E. POWELL and W. SEERING 1984 *Transactions of the ASME Journal of Vibration, Acoustics, Stress and Reliability in Design* **106**, 22–28. Multichannel structural inverse filtering.
16. W. J. KRZANOWSKI and P. KLINE 1995 *Multivariate Behavioral Research* **30**, 140–165. Cross-validation for choosing the number of important components in principal component analysis.
17. G. H. DUNTEMAN 1989 *Principal Components Analysis*. Beverly Hills, CA: SAGE Publications.
18. S. H. YOON and P. A. NELSON 1998 *ISVR Technical Report No*. 279, *University of Southampton*. Estimation of acoustic source strength by inverse methods. Part II Methods for choosing regularisation parameters.
19. S. H. YOON 1998 *Ph.D. thesis, University of Southampton*. Reconstruction of acoustic source strength distributions and their interactions by inverse techniques.
20. National Instrument 1996 *Instrumentation Reference and Catalogue*.
21. R. D. BLEVINS 1979 *Formulas for Natural Frequency and Mode Shape*. New York: Van Nostrand Reinhold Company.
22. N. A. HALLIWELL 1979 *Journal of Sound and Vibration* **62**, 312–315. Laser-doppler measurement of vibrating surfaces: a portable instrument.
23. K. R. HOLLAND and F. J. FAHY 1996 *Proceedings InterNoise* **96**, 2581–2584. Application of an area-integrating vibration velocity transducer.